UNCLASSIFIED SECRET

Report No. BMI-1200
C-86 Nuclear Rocket Engines
(M-3679, 19th Ed.)

This document consists of 60 pages,
No. 35 of 67 copies, Series A.

Contract No. W-7405-eng-92

CARBIDE COATINGS ON GRAPHITE

by

John M. Blocher, Jr.
Carl J. Ish
Don P. Leiter
Layne F. Plock
Ivor E. Campbell

Classification cancelled (or changed to UNCLASSIFIED)
by authority of Letter from Declassification Br. dated 11-6-58
by C.P. Boggess TiE, date 11-21-58

June 28, 1957

LEGAL NOTICE

This report was prepared as an account of Government sponsored work. Neither the United States, nor the Commission, nor any person acting on behalf of the Commission:

A. Makes any warranty or representation, expressed or implied, with respect to the accuracy, completeness, or usefulness of the information contained in this report, or that the use of any information, apparatus, method, or process disclosed in this report may not infringe privately owned rights; or

B. Assumes any liabilities with respect to the use of, or for damages resulting from the use of any information, apparatus, method, or process disclosed in this report.

As used in the above, "person acting on behalf of the Commission" includes any employee or contractor of the Commission, or employee of such contractor, to the extent that such employee or contractor of the Commission, or employee of such contractor prepares, disseminates, or provides access to, any information pursuant to his employment or contract with the Commission, or his employment with such contractor.

BATTELLE MEMORIAL INSTITUTE
505 King Avenue
Columbus 1, Ohio

SECRET
DECLASSIFIED UNCLASSIFIED
2-1

DISCLAIMER

This report was prepared as an account of work sponsored by an agency of the United States Government. Neither the United States Government nor any agency Thereof, nor any of their employees, makes any warranty, express or implied, or assumes any legal liability or responsibility for the accuracy, completeness, or usefulness of any information, apparatus, product, or process disclosed, or represents that its use would not infringe privately owned rights. Reference herein to any specific commercial product, process, or service by trade name, trademark, manufacturer, or otherwise does not necessarily constitute or imply its endorsement, recommendation, or favoring by the United States Government or any agency thereof. The views and opinions of authors expressed herein do not necessarily state or reflect those of the United States Government or any agency thereof.

DISCLAIMER

Portions of this document may be illegible in electronic image products. Images are produced from the best available original document.

Copy No.	*Distribution*
1	Aerojet-General Corporation (Thomas Beehan)
2	AF Plant Representative, Baltimore
3	AF Plant Representative, Long Beach
4	Air Research and Development Command (RDZPSP)
5	Air Technical Intelligence Center
6	ANP Project Office, Fort Worth
7	Albuquerque Operations Office
8	Armed Forces Special Weapons Project, Sandia
9	Armed Forces Special Weapons Project, Washington
10	Assistant AF Plant Representative, Downey
11-14	Atomic Energy Commission, Washington
15	Bureau of Ordnance
16	Bureau of Ordnance (SP-209)
17	Headquarters, Air Force Special Weapons Center
18-19	Los Alamos Scientific Laboratory
20	National Advisory Committee for Aeronautics, Cleveland
21	National Advisory Committee for Aeronautics, Washington
22	North American Aviation, Inc. (Missile Development Division)
23	Redstone Arsenal
24	San Francisco Operations Office
25-26	USAF Project RAND
27	U. S. Naval Ordnance Test Station
28-31	University of California Radiation Laboratory, Livermore
32	Western Development Division
33-34	Wright Air Development Center (WCOSI-3)
35-59	Technical Information Service Extension, Oak Ridge
60-67	Battelle Memorial Institute

DECLASSIFIED

TABLE OF CONTENTS

	Page
ABSTRACT	7
INTRODUCTION	7
Limiting-Pressure Determinations	8
Thermodynamic Treatment of Limiting-Pressure Data	9
Coating of Blowpipe Specimens	16
Coating of Uranium-Impregnated Specimens	29
Diffusion of Carbon in Carbides	34
ACKNOWLEDGMENT	38
REFERENCES	38
APPENDIX A	
APPARATUS AND PROCEDURE FOR LIMITING-PRESSURE DETERMINATIONS	41
APPENDIX B	
COATING OF BLOWPIPE SPECIMENS	53
Material	53
Apparatus	53
Typical Data	53
Atmospheric-Pressure Coater	57
APPENDIX C	
THERMODYNAMIC ANALYSIS OF PRESSURE RANGE FOR METAL-FREE CARBIDE FORMATION	59

DECLASSIFIED

2 - 2

CARBIDE COATINGS ON GRAPHITE

John M. Blocher, Jr., Carl J. Ish, Don P. Leiter,
Layne F. Plock, and Ivor E. Campbell

A method has been developed for the uniform coating of graphite tubes with carbides of niobium, tantalum, and zirconium by thermal decomposition of their respective halide vapors. Conditions of coating temperature and pressure are so chosen as to prevent the deposition of metal, but to permit the formation of the carbide as rapidly as carbon can diffuse to the surface. If the carbon diffusion can be made the rate-limiting step, the coating process becomes self-regulating and uniform thickness results. The limits of the temperature-pressure range have been determined experimentally for the thermal decomposition of zirconium iodide and of the chlorides and bromides of niobium, tantalum, and zirconium.

With the successful development of coating equipment and definition of conditions, 99 blowpipe test specimens were coated with uniform, continuous, and adherent layers of the carbides in three ranges of thickness, light (0.001 in.), medium (0.005 in.), and heavy (0.01 in.).

Determinations were maae of the coefficient for the diffusion of carbon in zirconium carbide as a function of temperature.

Exploratory work on small specimens of graphite impregnated with 7 w/o uranium indicated that the coating results were essentially unchanged, but that loss of uranium occurred. Means of avoiding the loss of uranium are discussed.

INTRODUCTION

The research described in this report was engendered by the problem of uniformly coating graphite with carbides of niobium, tantalum, and zirconium on the inside of long bores. Although other methods of coating were considered, vapor deposition offered the greatest promise of forming continuous, adherent coatings. However, as normally practiced, vapor deposition has the disadvantage that considerable attention must be given to the vapor-flow pattern to avoid nonuniformity. Adjustment of the vapor-flow pattern is practical in coating some shapes, but serious limitations are imposed in the case of small-bore tubing. For example, if the coating were to be formed in the usual manner[1] by the hydrogen reduction of a metal halide-hydrocarbon mixture, one would expect it to be thicker at the vapor-entrance end of the bore than at the vapor-exit end. The same difficulty would be encountered in the deposition of a layer of metal to be later converted to carbide by interdiffusion at elevated temperatures.

The multivalent character of the transition elements involved in this work holds the key to a method of avoiding nonuniformity by making the rate of formation of the coating dependent on the rate of diffusion of carbon from the base through the carbide coating. This can best be shown by example.

(1) References at end of text.

DECLASSIFIED 2-3

The thermal decomposition of zirconium iodide vapor at low pressures has long been used as a method of preparing high-purity zirconium metal.[2] The over-all reaction is $ZrI_4(g) \rightarrow Zr(s) + 4I(g)$. However, owing to the stability of the lower iodides, ZrI_3 and ZrI_2, reactions of the type $ZrI_4(g) + Zr(s) \rightarrow 2ZrI_2(g)$ may also occur. In fact, as the pressure of ZrI_4 is increased, reactions of the second type become more important and, as equilibrium calculations will show, at any given temperature there exists a limiting tetraiodide pressure below which zirconium will be deposited and above which metal will be consumed. This situation is general with the gaseous halides of the transition metals.

It can also be shown that a limiting pressure exists at a higher level for reactions of the type $ZrI_4(g) + C(s) \rightarrow ZrC(s) + 4I(g)$. Thus, by operating in the region above the limiting pressure for metal deposition and below the limiting pressure for carbide formation, one can avoid the deposition of metal and form only the carbide. Moreover, if the vapor-flow rate is made sufficiently high, the rate of formation of the coating becomes limited, not by kinetics or mass-transfer considerations at the vapor-carbide interface, but by the rate of diffusion of carbon through the carbide coating. Since the rate of diffusion is inversely proportional to the thickness of the coating, the thickness increase becomes self-regulating and independent of vapor-flow considerations over a wide range.

The research reported here was carried out to develop and apply this technique to the coating of blowpipe specimens for the University of California Radiation Laboratory at Livermore, California, where the protection of the graphite from high-temperature corrosion of certain gases was to be tested.

A twofold plan of attack was adopted, consisting of a fundamental and an engineering approach. In the fundamental program, the pressure-temperature limits for metal and carbide formation were to be determined along with such other information as might be applicable, while, in the engineering program, a specimen plater was to be developed having sufficient flexibility to be operable in the ranges indicated by the fundamental work.

Limiting-Pressure Determinations

The limiting pressures as functions of temperature were determined for metal and carbide formation by the thermal decomposition of zirconium iodide and of the chlorides and bromides of niobium, tantalum, and zirconium. Although it was not anticipated that all of these halides would be used in the coating of blowpipe specimens, data were obtained on their decomposition to provide the widest possible choice of conditions for the coating work. The iodides of niobium and tantalum were not considered, since it was predicted that, because of their low stability, formation of carbide in the absence of metal would have to be carried out in a temperature range so low as to make the rate of diffusion of carbon through the carbide impractically slow.

The technique of making these measurements is described in Appendix A. Briefly, it consisted of passing the metal halide vapor at controlled pressure over a resistively heated wire for metal deposition or a carbon rod for carbide formation, increasing the temperature of the deposition surface, and by monitoring the electrical resistance

2-4 DECLASSIFIED

(and/or total emission in the case of the carbides), determining the temperature at which the wire or rod showed neither growth nor attack. Although it was possible to establish a true equilibrium temperature in several instances, the limit was established in most cases as a somewhat uncertain boundary between points of deposition and of no deposition or attack.

The results of this work are shown in Figures 1, 2, and 3, where the limiting pressures in millimeters of mercury are plotted on a logarithmic scale against the temperatures in degrees centigrade on a scale linear with the reciprocal of absolute temperature. The experimental points are shown in Appendix A.

These graphs, showing the pressure-temperature ranges favorable to carbide formation and unfavorable to metal deposition, served as the basis for the choice of conditions for coating blowpipe specimens.

X-ray diffraction studies indicated that NbC, TaC, and ZrC were the principal carbides formed in the above work. However, although the monocarbide invariably formed adjacent to the graphite, it was possible, under pressure-temperature conditions toward the metal-deposition limit, to form mixtures of carbides (e.g., TaC and Ta_2C) and metal, and, in some cases, carbides with reduced lattice parameters, indicating possible defect lattices or ranges of homogeneity. Where liquid or solid solubility, or intermediate carbides exist in the carbide-metal system, such coatings would be expected to form at equilibrium at some point between the pressure-temperature limits for carbide and metal deposition. A study of the coating properties as a function of coating conditions would be profitable. Unfortunately, time did not permit the adoption of such a program.

Figures 4, 5, and 6 are photomicrographs of typical coatings obtained in these experiments on small ATJ-grade graphite rods. Although there are microscopic discontinuities in the coatings, they are considered to be continuous from a macroscopic standpoint.

It should be noted that, in these runs, the rate of vapor flow was probably insufficient to permit the coating rate to be controlled by diffusion of carbon through the carbide. The coating times given should be interpreted with this condition in mind.

The adherence characteristic of the coatings prepared in this work is attributed, at least in part, to the fact that the great throwing power evident in Figures 4, 5, and 6 locks the coating to surface irregularities. In all of the coatings prepared to date in the range 1900 to 2200 C, only one case of spalling was observed, and this was the result of oil vaporizing from a graphite adaptor which had been contaminated during machining. Thus, the carbides formed from carbon of the substrate were adherent without exception.

Thermodynamic Treatment of Limiting-Pressure Data

Since the existence of a limiting pressure in the thermal dissociation of a halide vapor requires the existence of a stable lower halide, it should be possible, in principle, to determine the nature and thermodynamic properties of the lower halides by properly analyzing the limiting-pressure data.

DECLASSIFIED 2-8

SECRET

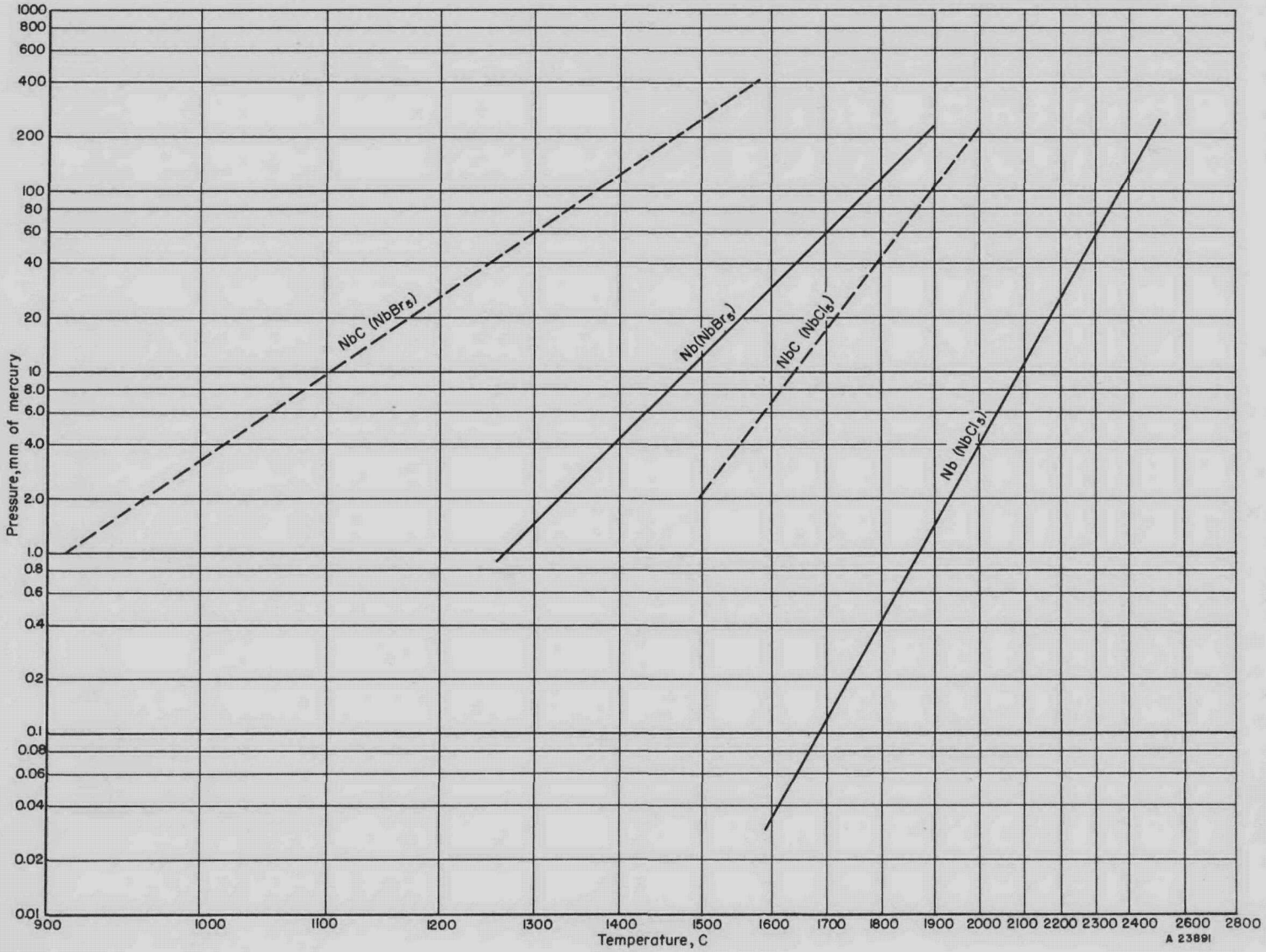

FIGURE 1. LIMITING PRESSURES FOR THE FORMATION OF NbC ON CARBON (DASHED LINE) AND OF NIOBIUM (FULL LINE) BY THERMAL DECOMPOSITION OF $NbCl_5$ AND $NbBr_5$

SECRET

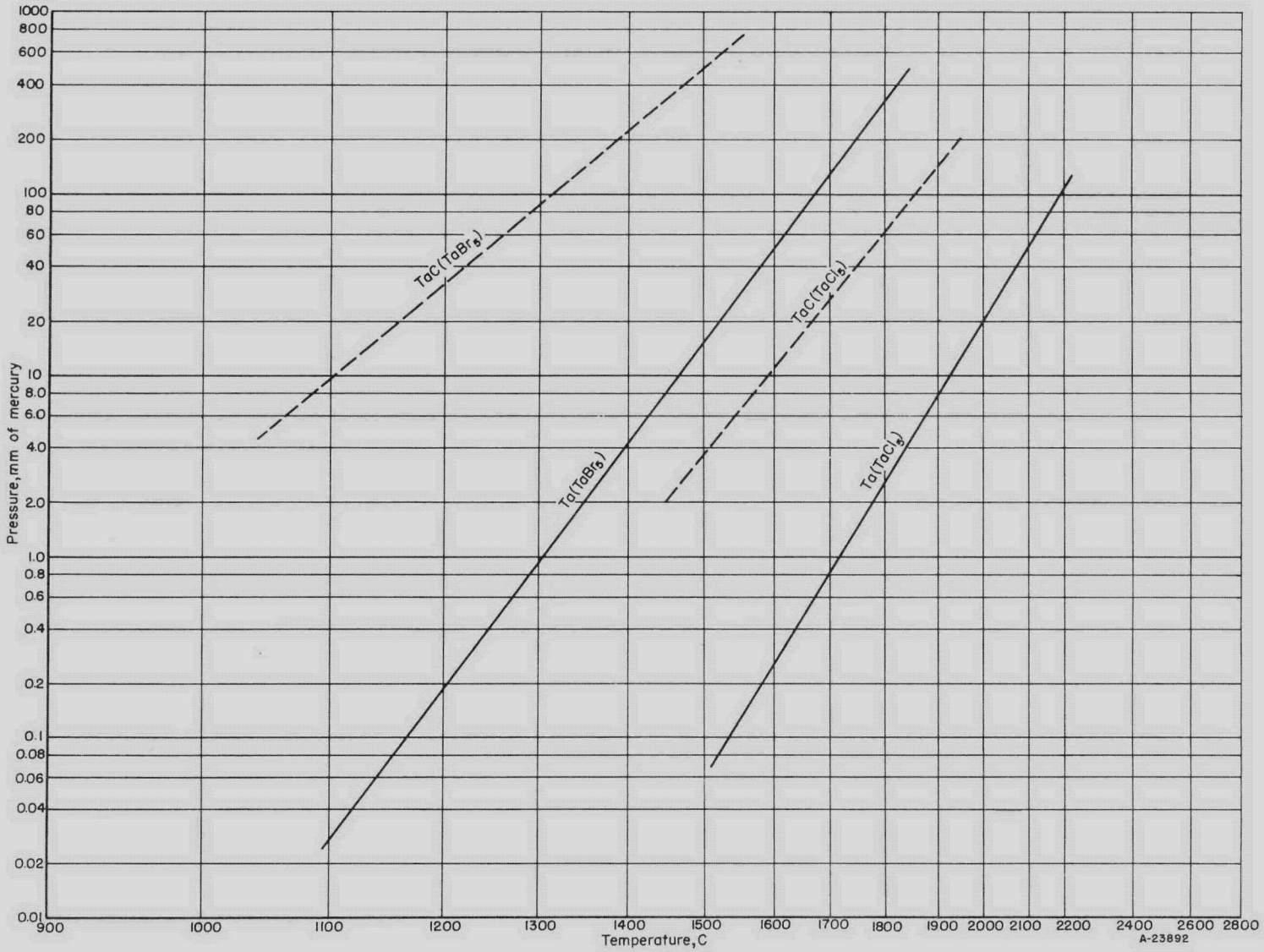

FIGURE 2. LIMITING PRESSURES FOR THE FORMATION OF TaC ON CARBON (DASHED LINE) AND OF TANTALUM (FULL LINE) BY THERMAL DECOMPOSITION OF $TaCl_5$ AND $TaBr_5$

SECRET

SECRET

Declassified

SECRET

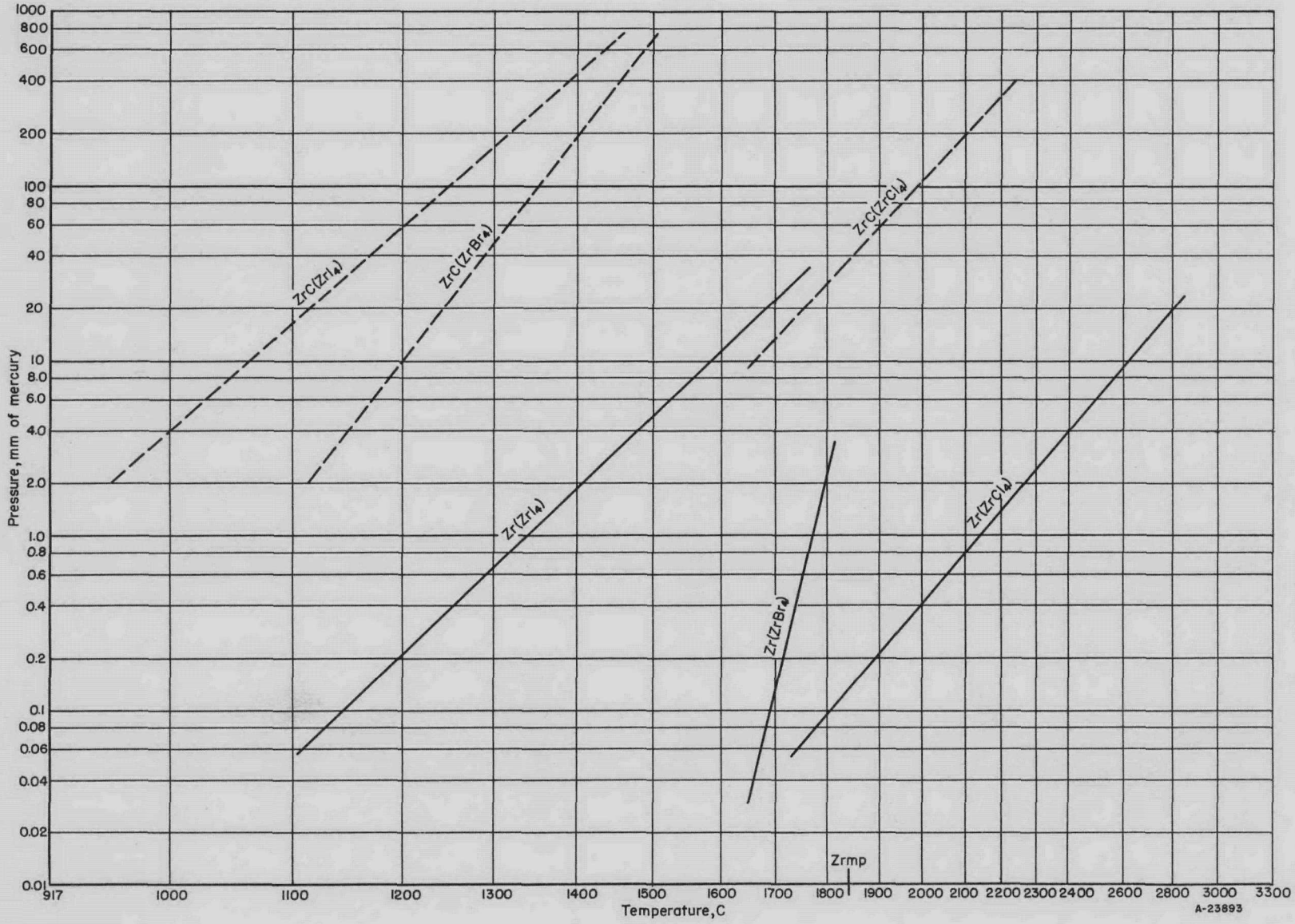

FIGURE 3. LIMITING PRESSURES FOR THE FORMATION OF ZrC ON CARBON (DASHED LINE) AND OF ZIRCONIUM (FULL LINE) BY THERMAL DECOMPOSITION OF $ZrCl_4$, $ZrBr_4$, AND ZrI_4

SECRET

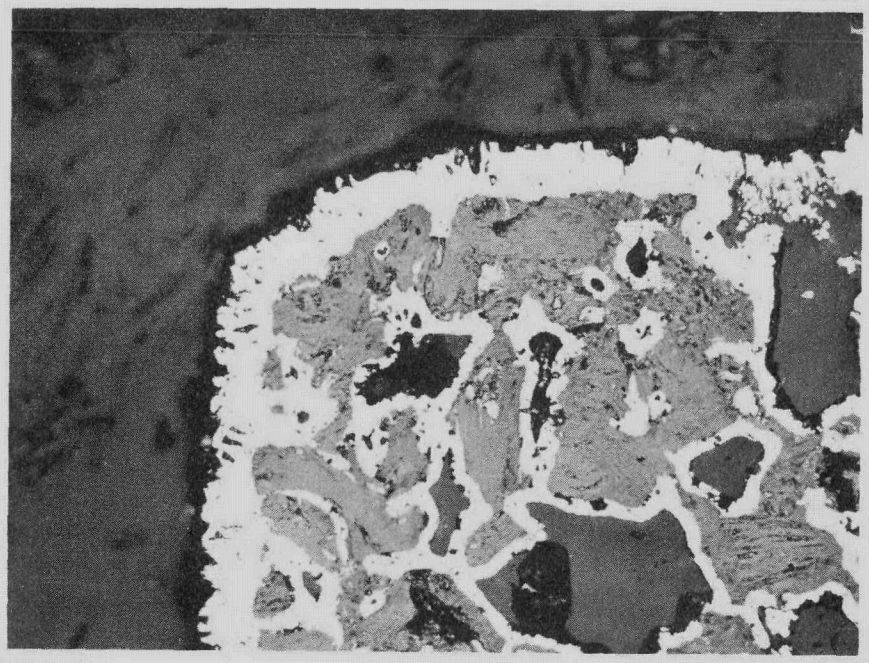

250X N41599

FIGURE 4. NIOBIUM CARBIDE COATING ON ATJ GRAPHITE FORMED IN 45 MIN BY THERMAL DECOMPOSITION OF $NbBr_5$ AT 1200 TO 1500 C AT 100 MM OF MERCURY

Run 12644-25.

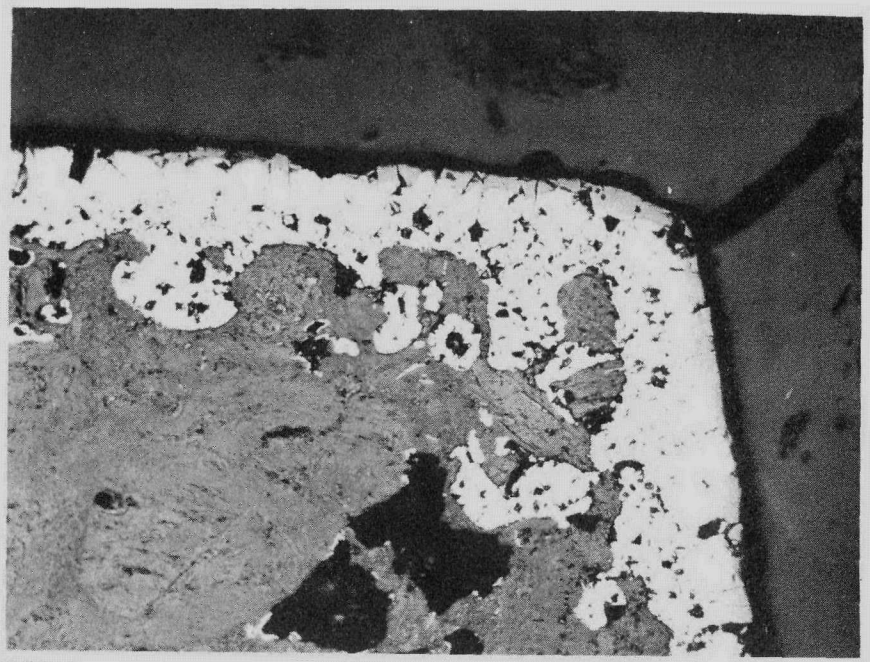

250X N41600

FIGURE 5. TANTALUM CARBIDE COATING ON ATJ GRAPHITE FORMED IN 10 MIN BY THERMAL DECOMPOSITION OF $TaCl_5$ AT 1890 TO 2000 C AT 48 MM OF MERCURY

Run 12010-59.

DECLASSIFIED 2-9

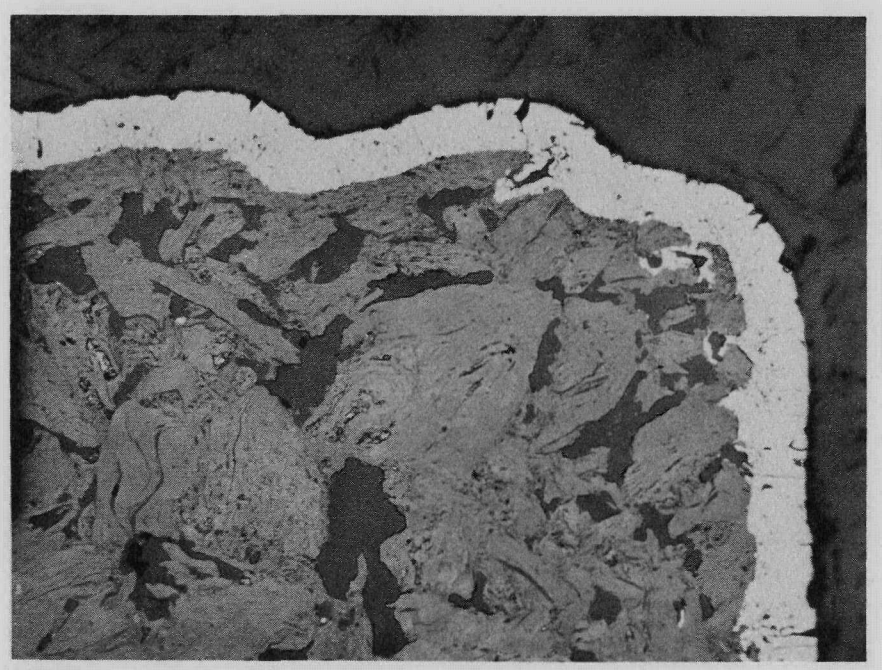

250X N41601

FIGURE 6. ZIRCONIUM CARBIDE COATING ON ATJ GRAPHITE FORMED IN 30 MIN BY THERMAL DECOMPOSITION OF $ZrCl_4$ AT 1900 TO 2100 C AT 12 MM OF MERCURY

Run 12010-38.

2-10

Attempts have been made to treat the data quantitatively, but with little success within the time limit imposed by justifying the effort. Even the treatment of the simplest situation is beyond the scope of this report, and the simple model is not entirely satisfactory.

It is possible, however, to obtain from thermodynamic considerations a semi-quantitative picture of the range of pressure between metal deposition and carbide formation which is useful (see Appendix C).

On the assumption that dissociation has progressed to the point that the vapor at the limiting pressure consists solely of halogen atoms and molecules of the lower halide, it can be shown that the following relation holds:

$$\log P_{MC}/P_M = \frac{-\Delta F_{MC}}{(n-1)2.303RT},$$

where

P_{MC} = limiting pressure for carbide formation

P_M = limiting pressure for metal formation

ΔF_{MC} = free energy of formation of the carbide MC

T = temperature, K

n = number of halogen atoms per atom of metal in the lower halide.

The carbides of interest in this work have free energies of formation of -35 ±5 kcal per mole[3] in the temperature range 1100 to 2000 C. Thus, if the trihalide is the stable gaseous species, the limiting pressures for metal and carbide formation should differ by 2.6 log cycles at 1200 C, 2.20 log cycles at 1600 C, and 1.68 log cycles at 2000 C. If the dihalide is the stable species, the above values are doubled.

It can be seen from Figures 1, 2, and 3 that these differences are of the right order and that the convergence of the limiting pressures with increasing temperature is consistent with the analysis.

Another interesting relation derived from the simple picture described above is the fact that the slope of the log P_M versus 1/T line gives directly (on multiplying by -2.303R) the heat of the reaction $MX_2(g) = M(s) + 2X(g)$ or one-half of the heat of reaction

$$MX_3(g) = M(s) + 3X(g),$$

depending on whether the di- or trihalide is the existing stable species.

In the cases of tantalum and niobium, the slopes (or heats of dissociation) are greater for the chloride than for the bromide as would be predicted. The data for $ZrBr_4$ are out of line with the chloride and iodide, however, and would make an interesting subject for study. On the basis of the simple analysis described above, this

DECLASSIFIED 2-11

reversal indicates that, in the case of $ZrBr_4$ decomposition, the lower valent stable species is the dihalide rather than the trihalide, the indicated form for chloride and iodide.

Coating of Blowpipe Specimens

The blowpipe test specimens to be coated with the carbides of niobium, tantalum, and zirconium consisted of tubes of ATJ graphite, 0.75 in. in OD, 0.25 in. in ID, and about 18 in. long, with a shouldered fitting at one end and a ball-and-socket fitting at the other. Initially, it was planned that only the inside bore be coated, but arrangements were made later to coat both the inside and outside surfaces.

The shape of these specimens makes them admirably suited to resistance heating. However, it was necessary to use long adaptors of similar cross section to reduce conductive heat loss from the ends of the specimens. Radiative heat loss was reduced by a shielding capsule consisting of two concentric tubes of graphite with crushed graphite in the annulus. The inner tube of the shielding capsule also served to direct the vapor flow around the specimens.

Figure 7 is a general view of the equipment used in most of the coating work* showing one unit ready for operation and the other partially assembled. Operation of the plating units can be understood by reference to Figure 8. The entire assembly is contained in a water-cooled vacuum-tight tank, which can be outgassed and then subjected to an automatically controlled back pressure of inert gas. The internal assembly, consisting of a resistively heated graphite vaporizer, specimen and adaptors, and condenser is so arranged that the vaporizer takes the weight of the assembly when it rests on the bottom of the vacuum tank, and the specimen is free to expand on heating. Electrical connections to the vaporizer are made through the vacuum tank to the bottom of the vaporizer and to the stainless steel plate common to the vaporizer and the lower specimen adaptor. Connection to the top of the specimen is made at the plate holding the condenser. The heavy currents required are conducted to the electrode plates by water-cooled copper tubing which is coiled for flexibility. Separate power supplies are provided for the vaporizer and specimen as described in Appendix C.

Briefly, the operation consists of assembling the unit, inserting the charged vaporizer at the last moment before closure, evacuating the tank, setting the back pressure at a predetermined value, bringing the specimen up to temperature, and then heating the graphite vaporizer on a predetermined power schedule to vaporize the halide at an appropriate rate.

The proper balance of vapor flow through and around the specimen was achieved by optimizing the relative sizes of the axial and radial holes in the adaptors.

In the earlier work, when only the bore of the specimen was being coated, it was possible to measure the specimen temperature by sighting an optical pyrometer through the view port on the wall of the tank and a hole in the shielding capsule. When it became necessary to coat both the outside and inside of the specimens, the sight hole was closed and the Lavite insulating caps at the top and bottom of the capsule were made

*An earlier coating unit used in Runs 11661-50-1LM through 12416-47-19LF is described in Appendix B.

2-12 DECLASSIFIED

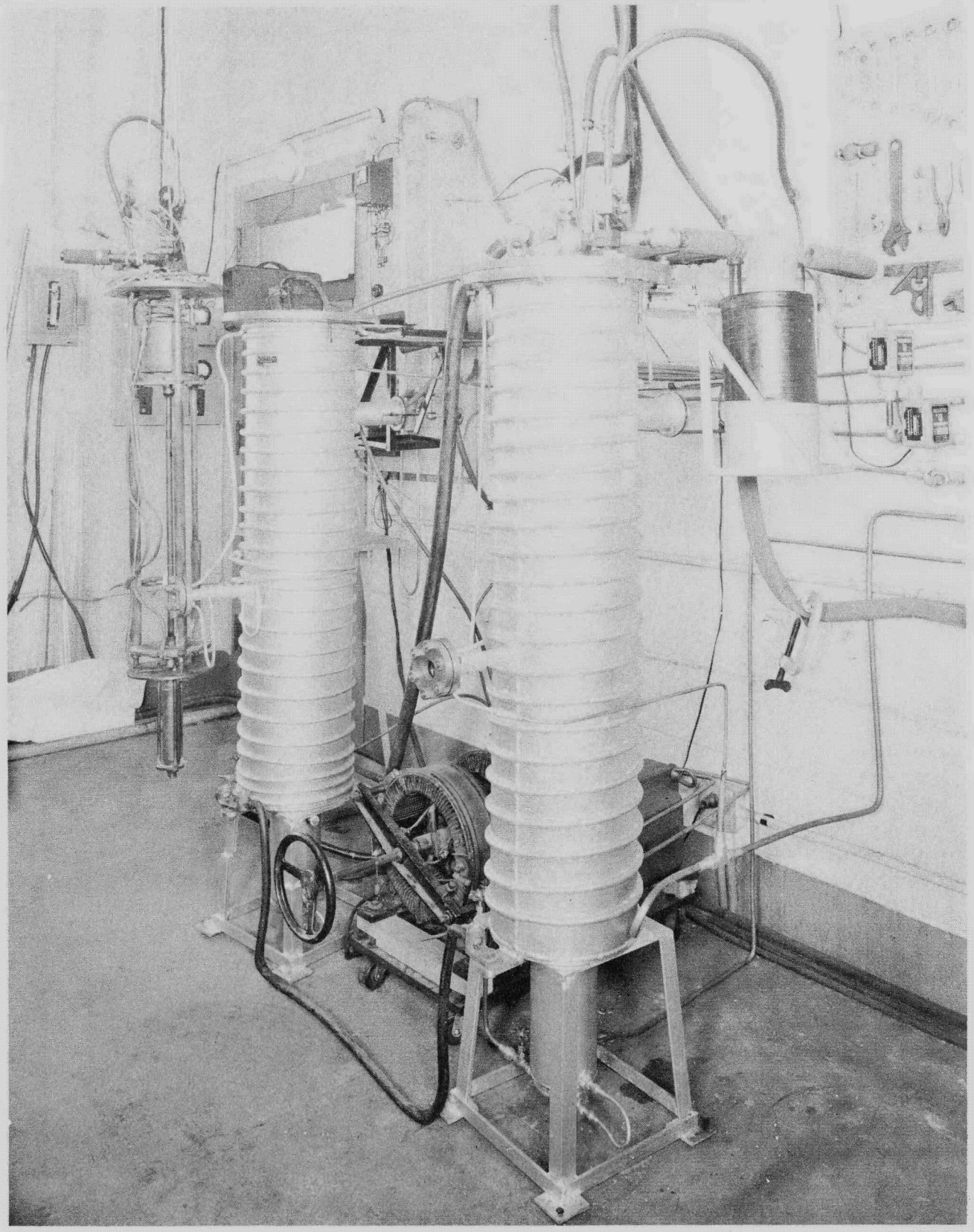

N39178

FIGURE 7. COATING EQUIPMENT FOR BLOWPIPE SPECIMENS

DECLASSIFIED 2-13

close fitting to minimize escape of vapor and to direct part of the vapor flow from the radial holes in the bottom adaptor around the specimen and into the radial holes in the top adaptor. Under these conditions, the specimen temperature was estimated by previously determined correlations with heating current and temperature of the outside wall of the insulating capsule.

Figure 9 shows an uncoated specimen, a set of adaptors, and specimens coated in 1 hr at about 2000 C with NbC, TaC, and ZrC from the chlorides at 50, 100, and 5 mm of mercury, respectively, the conditions finally adopted for coating most of the specimens.

Figures 10, 11, and 12 are reproductions of the X-radiographs of the above specimens. To obtain the metal-equivalent thickness of the coatings, the radiograph of the specimen was compared with that of a metal-foil step gage, by means of a densitometer. Figure 13 gives the corresponding densitometer traces showing metal-equivalent thicknesses of 7 ± 1.5 mils of niobium, 3 ± 0.7 mils of tantalum, and 2 ± 0.5 mils of zirconium.

Since the ratios of the densities of metal[4] to monocarbide[5] for niobium, tantalum, and zirconium are 1.092, 1.14, and 1.01, respectively, the carbide thicknesses would be a little greater than the values given above. The factors influencing the accuracy of this method of measurement have not been fully evaluated. However, in the few cases where the coating thickness was also measured by microscopic examination, the agreement was within 25 per cent.

The gradient in coating thickness is due to temperature gradients in the specimen. Contact resistance at the junction of the adaptor and specimen may account for the thicker coating at the ends. Other variations are attributable to specimen inhomogeneity. The resistance per unit length as a function of distance along the specimen axis was measured for all specimens prior to coating. Those showing greater than ±10 per cent variation were discarded.

Better temperature compensation at the ends of the specimen may be obtainable by further alteration of the adaptor geometry.

Figures 14, 15, and 16 are photomicrographs of typical cross sections showing the continuity and general structure of the blowpipe-specimen coatings. The difference in appearance of the coatings shown is significant. The outward appearance of the specimens is consistent with the microstructure, in that NbC- and ZrC-coated specimens are smooth and bright* while the TaC coatings are a matte-gold, indicating a rough surface.

It can be seen from the phase diagrams in Figure 17 that at coating temperatures of 2000-2200 C, ZrC and NbC coatings[6] are formed above the solidus in the metal-carbide system, whereas, TaC is formed below the solidus[7]. It is probable that ZrC and NbC form by crystallization from a liquid film at the outer surface of the coating, leading to a denser carbide.

It is interesting to note that X-ray diffraction measurements show only the monocarbides in the blowpipe-specimen coatings.

*ZrC is silvery. NbC is silvery with a pink tinge.

2-14

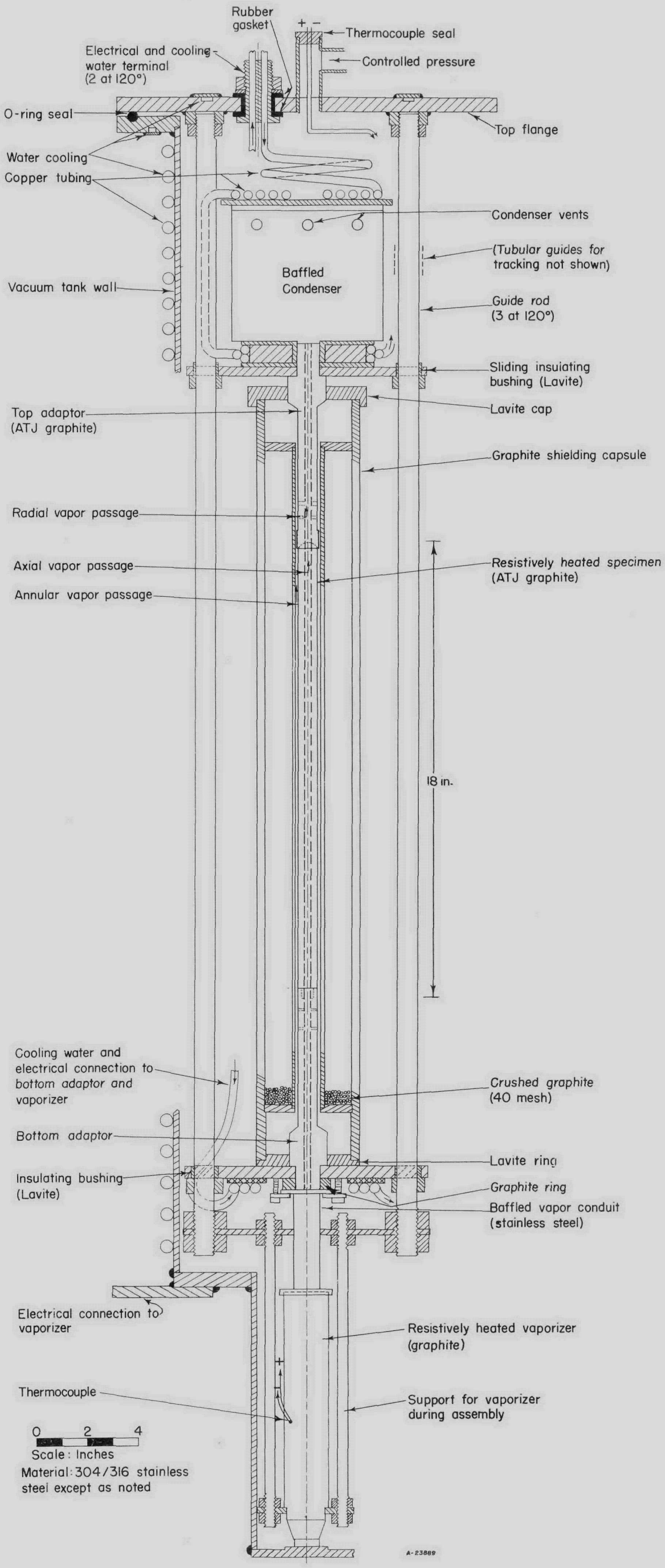

FIGURE 8. SPECIMEN COATER

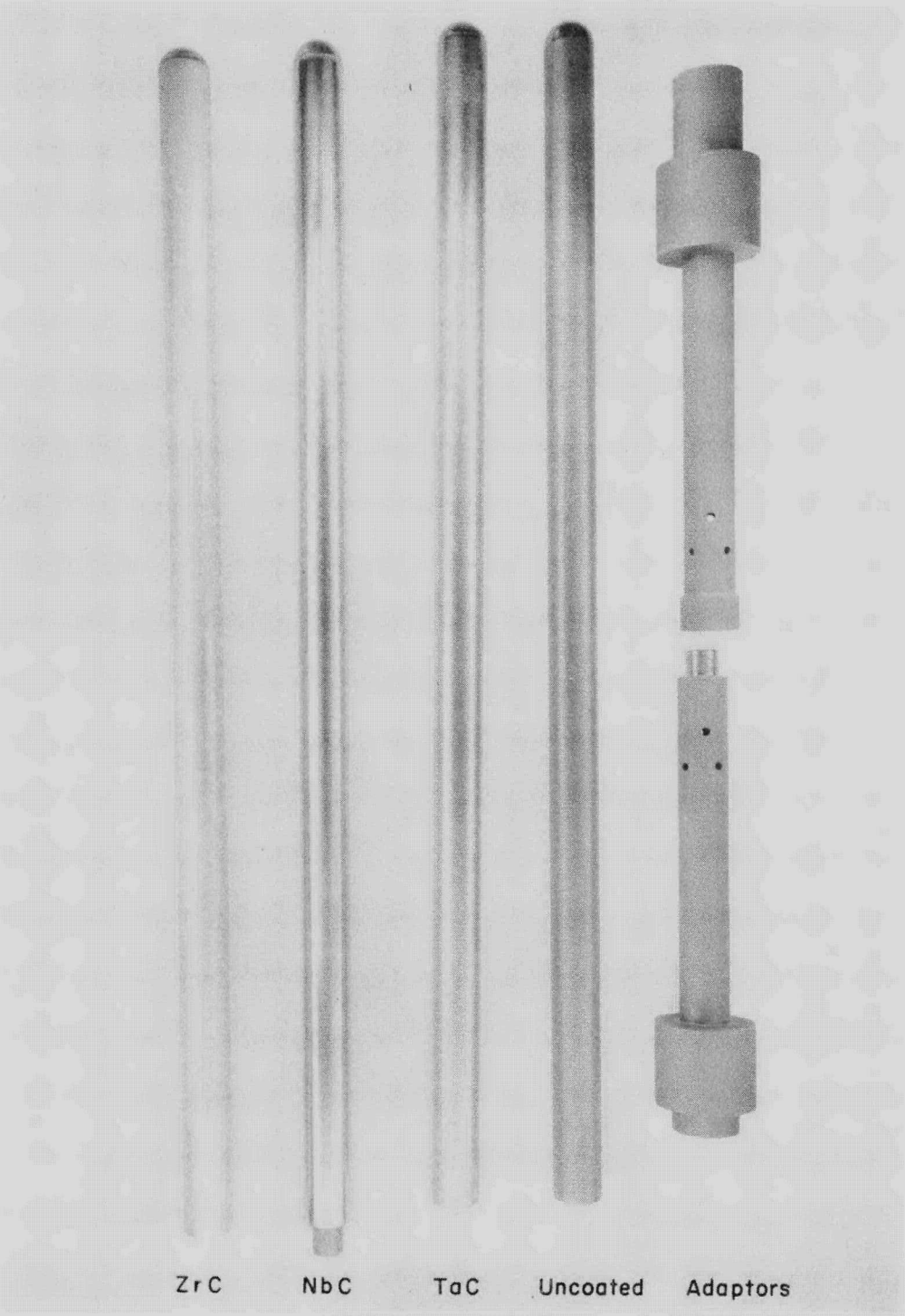

N41077

FIGURE 9. COATED AND UNCOATED BLOWPIPE SPECIMENS AND A SET OF ADAPTORS

TaC coated, Run 13331-19-75LF.
NbC coated, Run 13331-28-78LM.
ZrC coated, Run 13331-73-93LF.

DECLASSIFIED 2-16

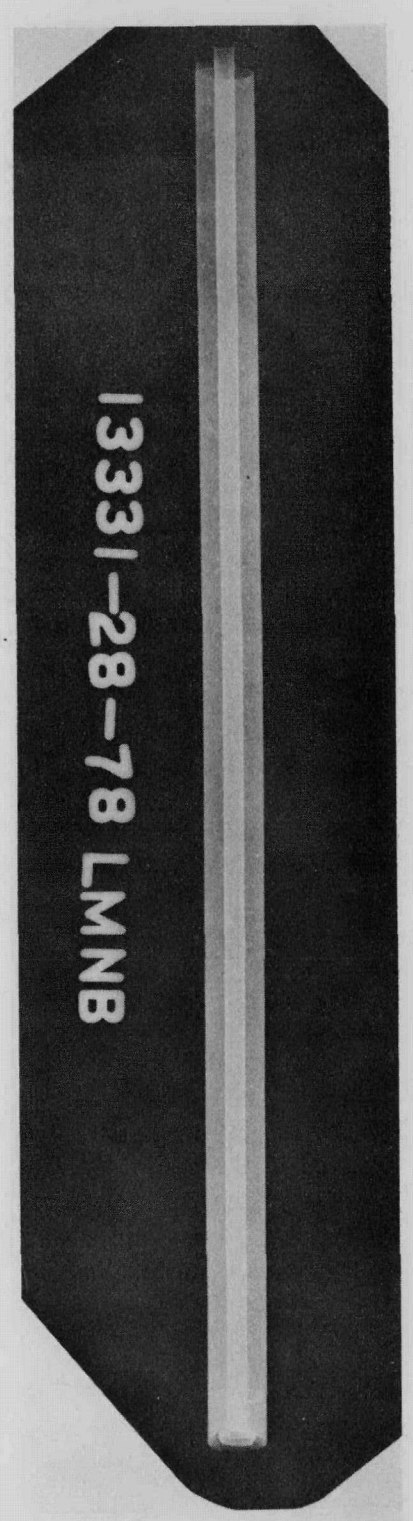

N41147

FIGURE 10. RADIOGRAPH OF NbC-COATED SPECIMEN

Run 13331-28-78LM. Coated by thermal decomposition of $NbCl_5$.

Note: Radiograph taken with portion of adaptor adhering to right end of specimen.

2-17

DECLASSIFIED

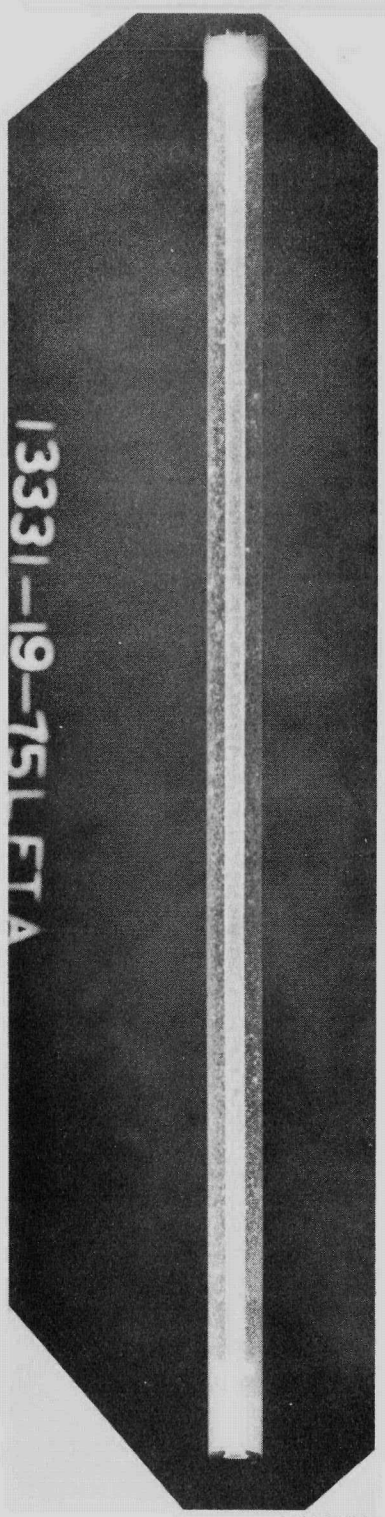

N41147A

FIGURE 11. RADIOGRAPH OF TaC-COATED SPECIMEN

Run 13331-19-75LF. Coated by thermal decomposition of $TaCl_5$.

Note: Radiograph taken with portions of the adaptors adhering to the ends of the specimen.

DECLASSIFIED

2-18

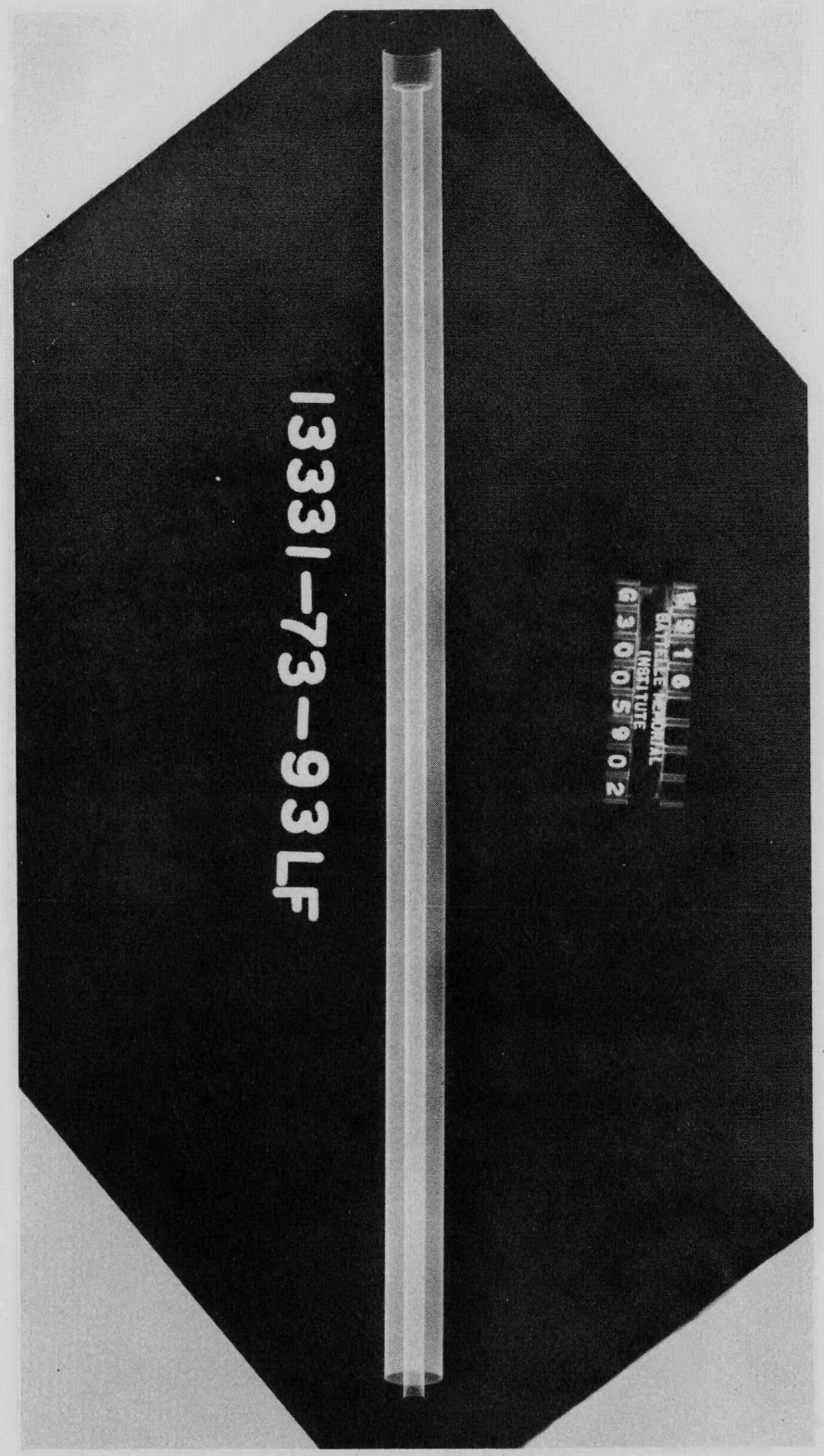

N41148

FIGURE 12. RADIOGRAPH OF ZrC-COATED SPECIMEN

Run 13331-73-93LF. Coated by the thermal decomposition of $ZrCl_4$.

2-19

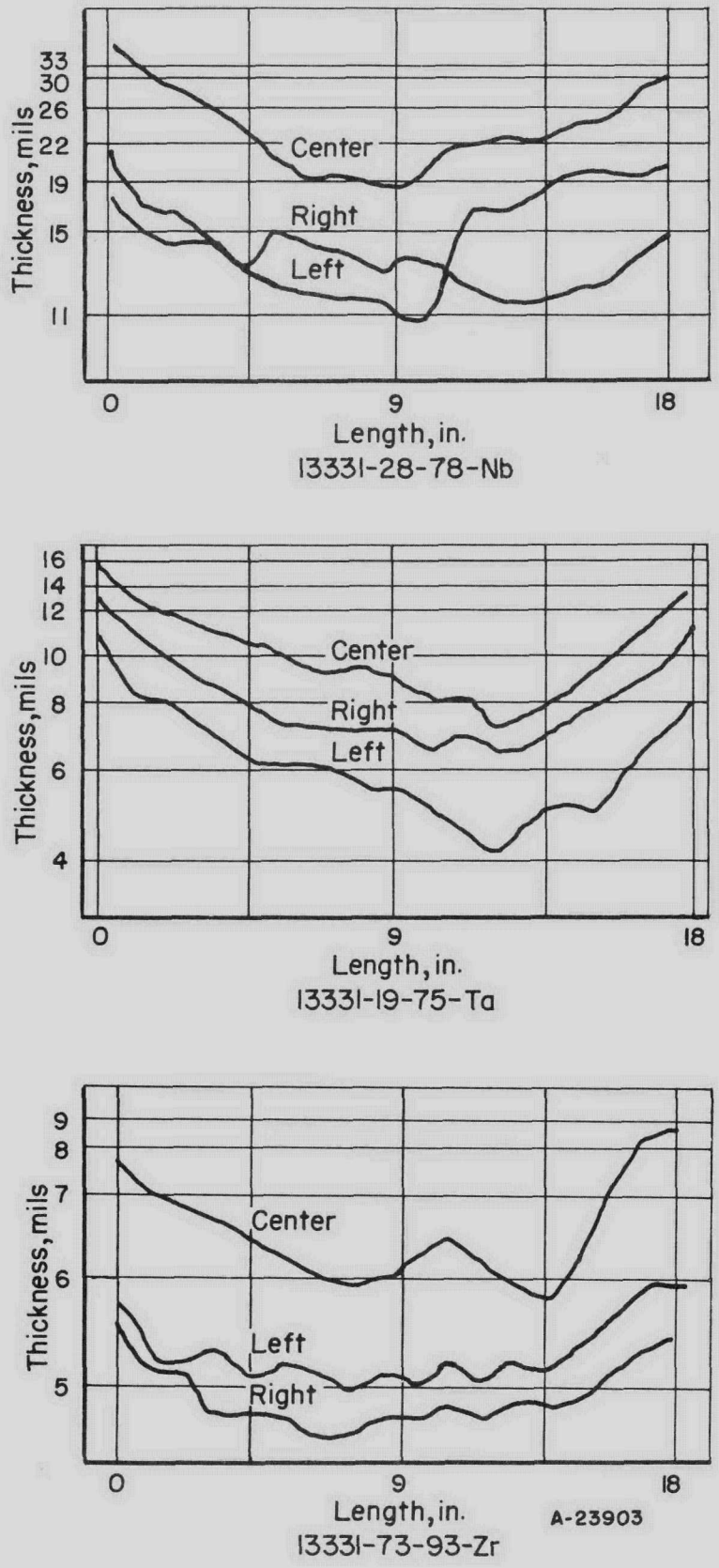

FIGURE 13. DENSITOMETER TRACES

DECLASSIFIED

2-20

500X N41101

FIGURE 14. NIOBIUM CARBIDE COATING ON ATJ GRAPHITE FORMED BY THERMAL DECOMPOSITION OF NIOBIUM PENTACHLORIDE

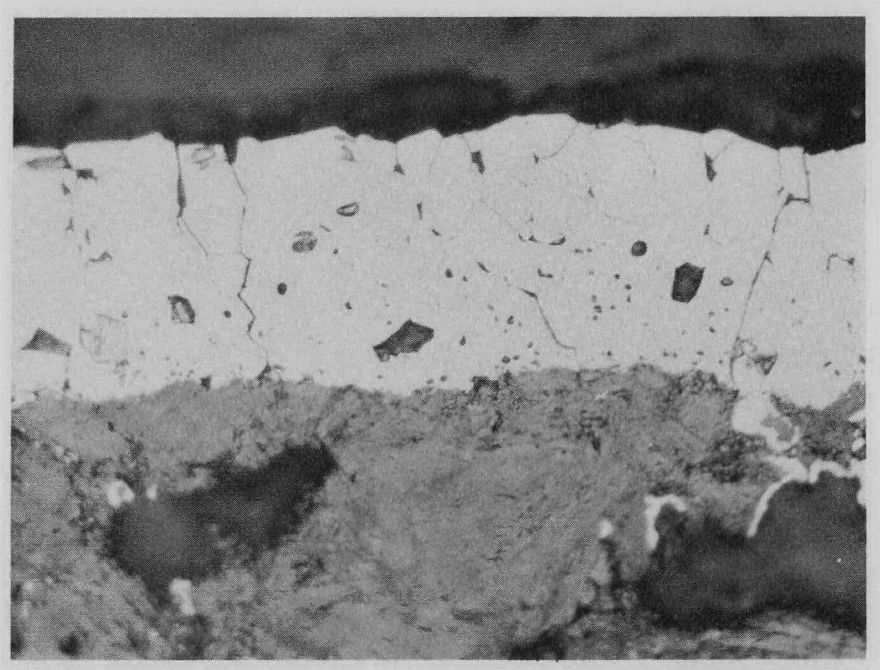

500X N41100

FIGURE 15. TANTALUM CARBIDE COATING ON ATJ GRAPHITE FORMED BY THERMAL DECOMPOSITION OF TANTALUM PENTACHLORIDE

2-21

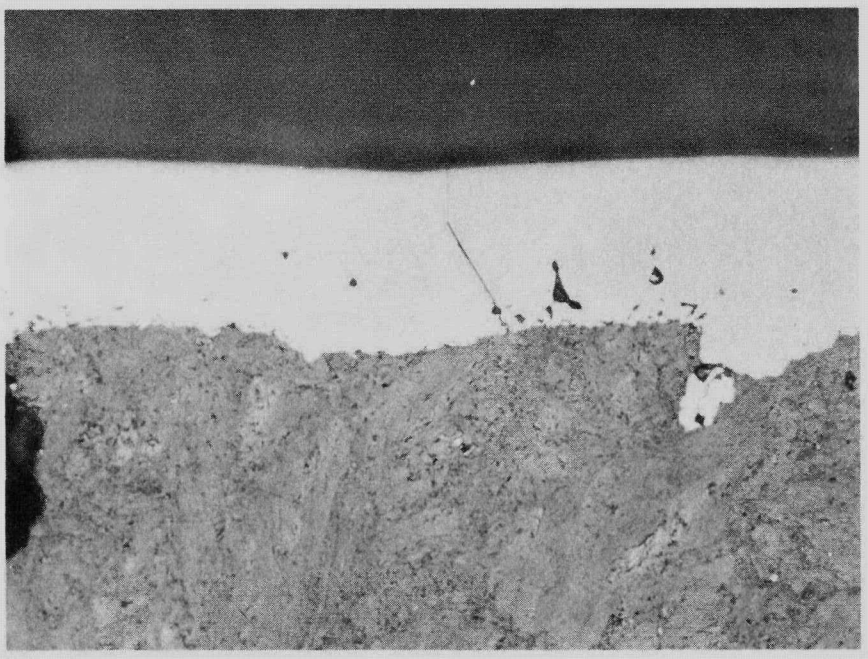

500X N41102

FIGURE 16. ZIRCONIUM CARBIDE COATING ON ATJ GRAPHITE FORMED BY THERMAL DECOMPOSITION OF ZIRCONIUM TETRACHLORIDE

DECLASSIFIED 2-22

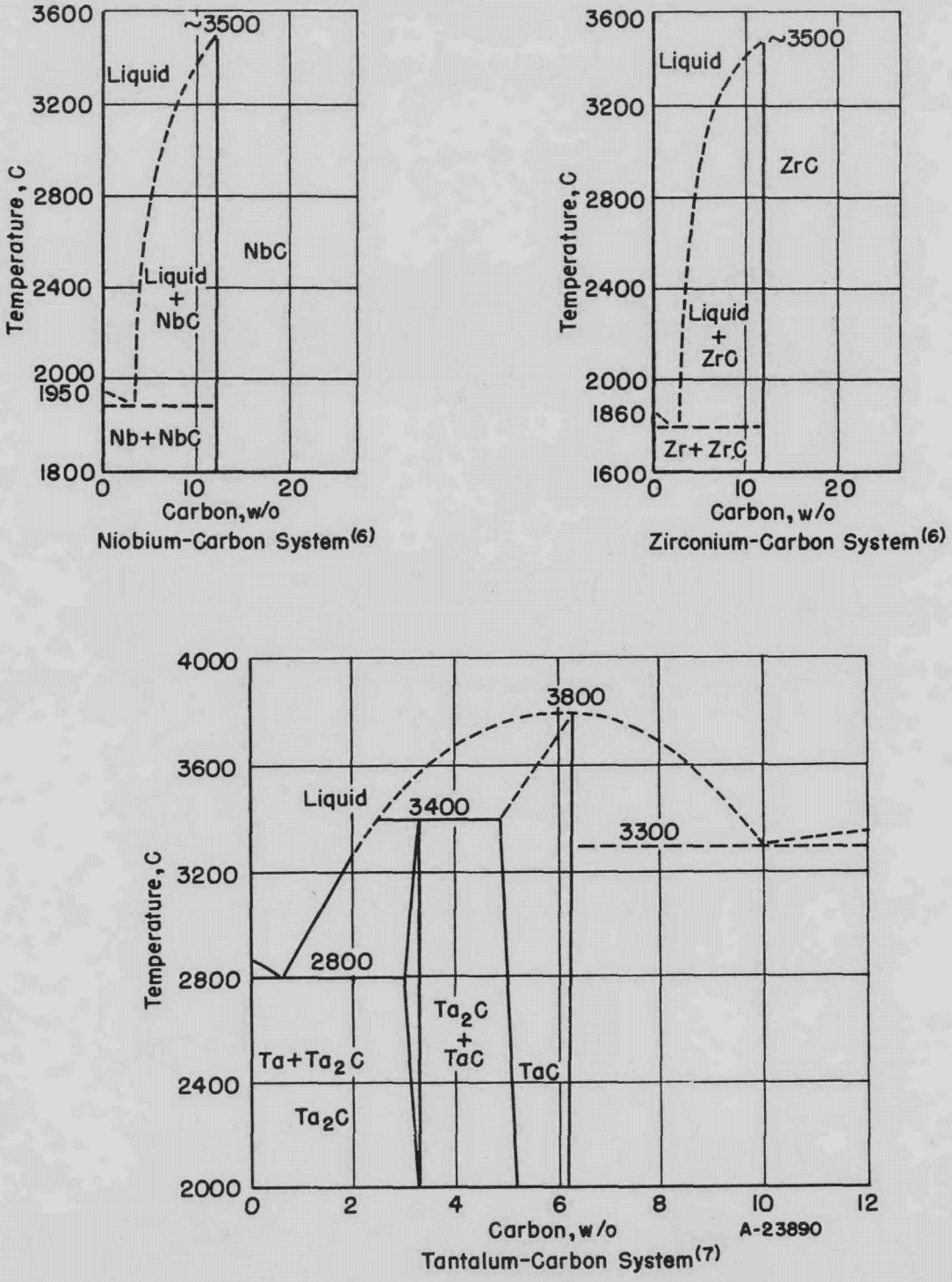

FIGURE 17. PHASE DIAGRAMS FOR THE NIOBIUM-CARBON, TANTALUM-CARBON, AND ZIRCONIUM-CARBON SYSTEMS

2-23

When the proper coating conditions were determined and the equipment had been developed, specimens were routinely coated at a rate of two or three per day.

A total of 99 useful specimens was coated with the three carbides in various thicknesses ranging from 0.5 to 20 mils.

Coating of Uranium-Impregnated Specimens

Uranium-impregnated ATJ graphite specimens were coated to test the effect of the presence of uranium on the resultant coating and to determine the extent to which uranium is leached from the specimens in the coating process.

Six rods of ATJ graphite, 3/32 in. in diameter, were sent to UCRL where they were solution impregnated with about 7 w/o uranium and fired to form the carbide. The specimens were coated as received in the apparatus described in Appendix A. Vaporization of the halide was brought to a steady state before the specimen was heated to the coating temperature of 2000 to 2070 C.

In three cases, the halide condensate from the coating operation was collected and analyzed for total uranium to determine the extent of leaching.

Table 1 gives the coating conditions and results.

TABLE 1. COATING OF URANIUM-IMPREGNATED SPECIMENS

Specimen	Halide	Pressure, mm of mercury	Uranium Content, mg		Loss, per cent
			Initial[a]	Condensate	
L-1	$ZrCl_4$	6.0	--	--	--
L-2	$ZrCl_4$	5.0	58	37.2	64
L-3	$NbCl_5$	49.5	56	37.9	67.5
L-4	$NbCl_5$	50.0	--	--	--
L-5	$TaCl_5$	106.5	53	50.4	95
L-6	$TaCl_5$	102.5	--	--	--

(a) UCRL analysis.

Table 2 gives the results of X-ray diffraction examination of the coatings.

DECLASSIFIED

TABLE 2. CONSTITUTION OF COATINGS ON URANIUM-IMPREGNATED GRAPHITE

Specimen	Phase	Intensity	Parameter, A	Remarks
L-2	Zr	Faint		
	ZrC	Strong	4.692(a)	--
L-4	NbC	Strong	4.467(a)	--
	Cubic	Medium faint	4.45	Carbon deficient ?
	Nb_2C (?)	Medium faint		
L-5	TaC	Very strong	4.55(a)	--
	TaC	Medium faint	4.40	Carbon deficient ?
	Ta_2C	Very faint		

(a) Schwarzkopf[5] gives a = 4.685, 4.46, and 4.55 A for face-centered-cubic ZrC, NbC, and TaC, respectively.

Figures 18, 19, and 20 compare the coatings with samples obtained on unimpregnated graphite (previously pictured in Figures 14, 15, and 16).

Comparison of the photomicrographs reveals the similarity of the coatings, with a somewhat greater concentration of voids and fissures present in the coatings of the impregnated specimens. However, other coatings such as those pictured in Figures 4, 5, and 6 show varying concentrations of voids. Thus, it is not possible, without further study under controlled conditions, to assess accurately the effect of the presence of uranium on the resultant coating.

The loss of uranium, presumably by the reduction of the halide vapors, is the most significant result of these experiments. Some leaching was expected. However, loss of this magnitude was surprising. Since it is understood that the uranium concentration was greatest at the surface of these solution-impregnated samples, the leaching effect would be expected to be more drastic here than with graphite, which is homogeneously loaded with uranium during its manufacture.

The leaching of uranium from uniformly loaded graphite was tested with samples resulting from longitudinally quartering a tube supplied by the Los Alamos Scientific Laboratory. The specimens were in the form of rods of roughly triangular cross section, about 3/32 in. on a side.

The uranium content of one of the quarters, 7.2 w/o, was taken as the original loading of the other three. Coating conditions and results are given in Table 3. The coating thickness was not measured in this series of experiments. However, the coating appeared to be normal and about 2 to 5 mils in thickness.

2-25

DECLASSIFIED

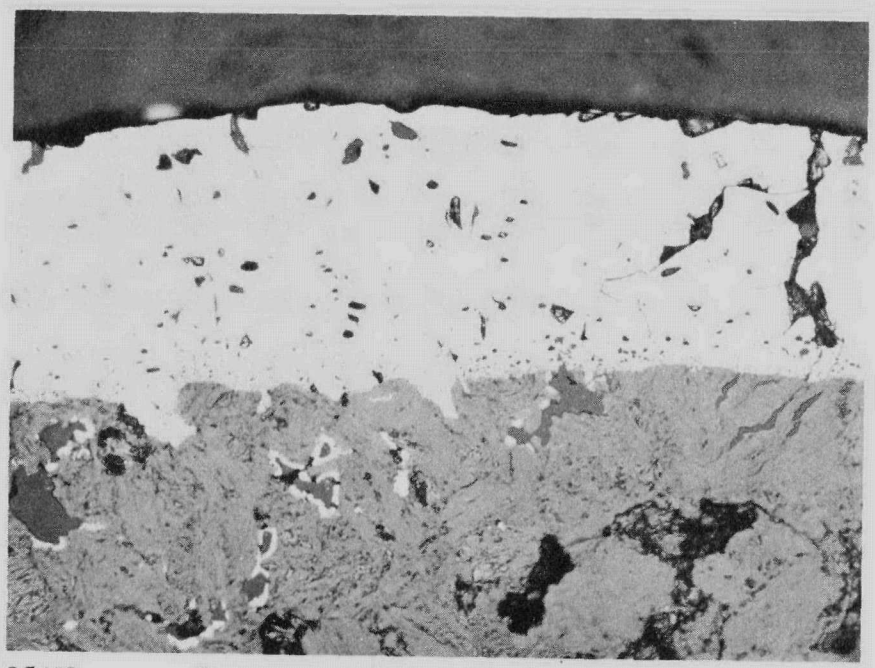

250X Impregnated With 7 w/o Uranium N41047

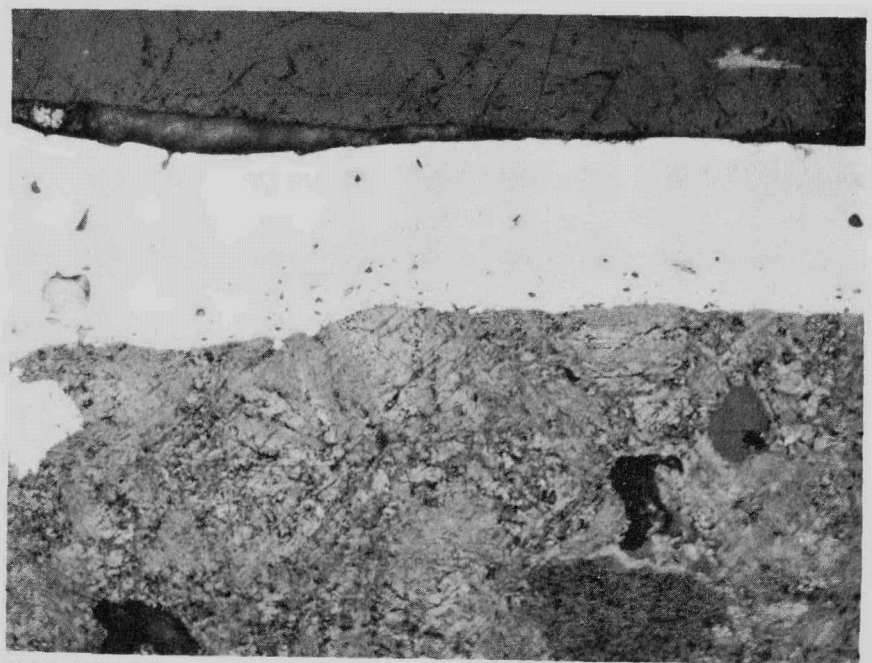

500X Unimpregnated N41101

FIGURE 18. NbC COATINGS ON ATJ GRAPHITE

DECLASSIFIED 2.26

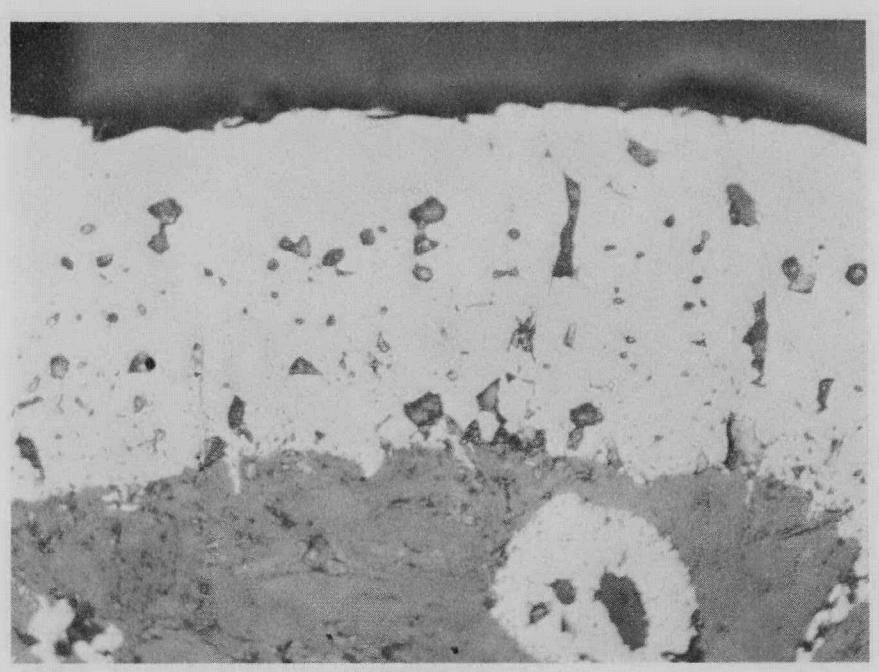

500X Impregnated With 7 w/o Uranium N41049

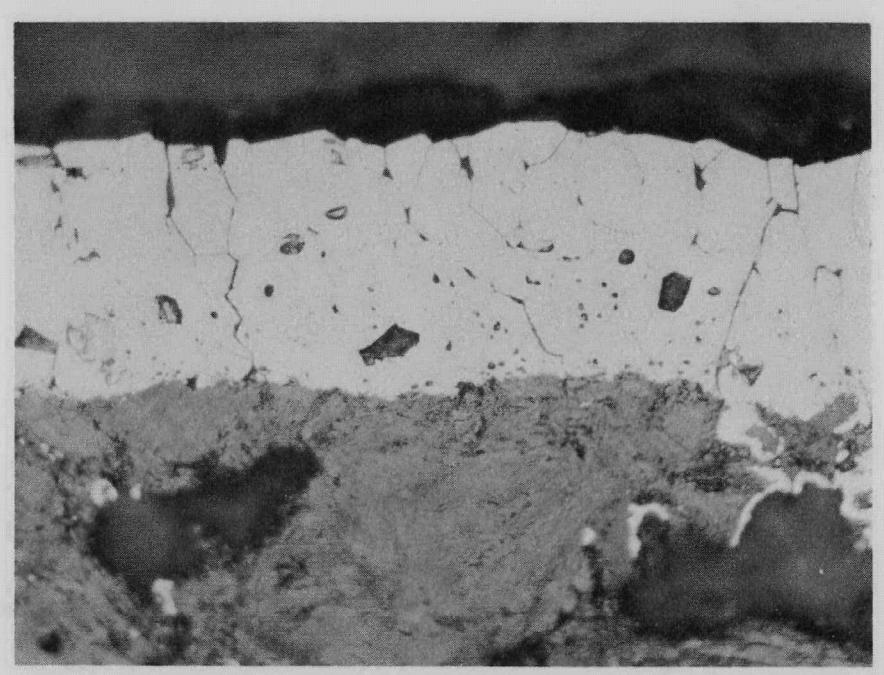

500X Unimpregnated N41100

FIGURE 19. TaC COATINGS ON ATJ GRAPHITE

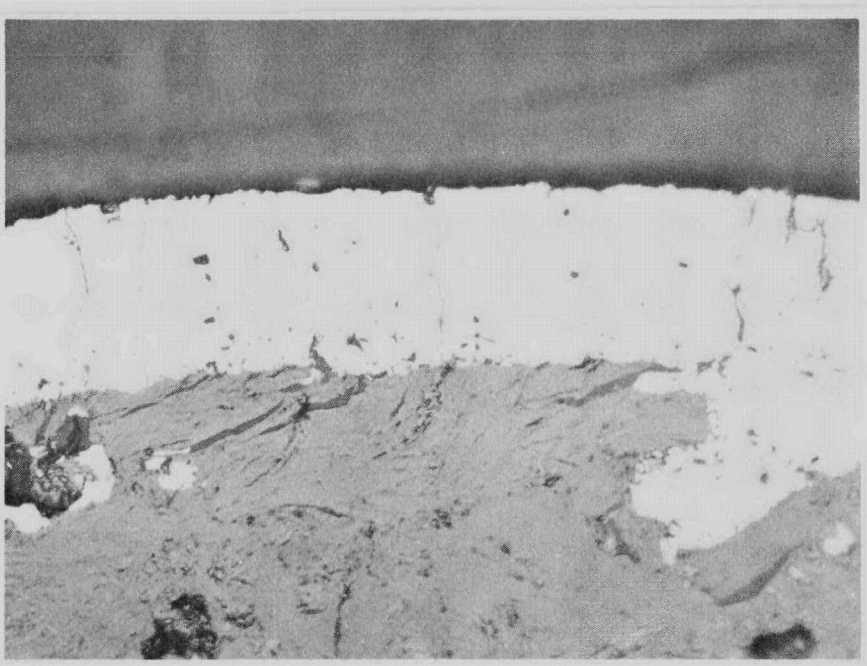

250X Impregnated With 7 w/o Uranium N41046

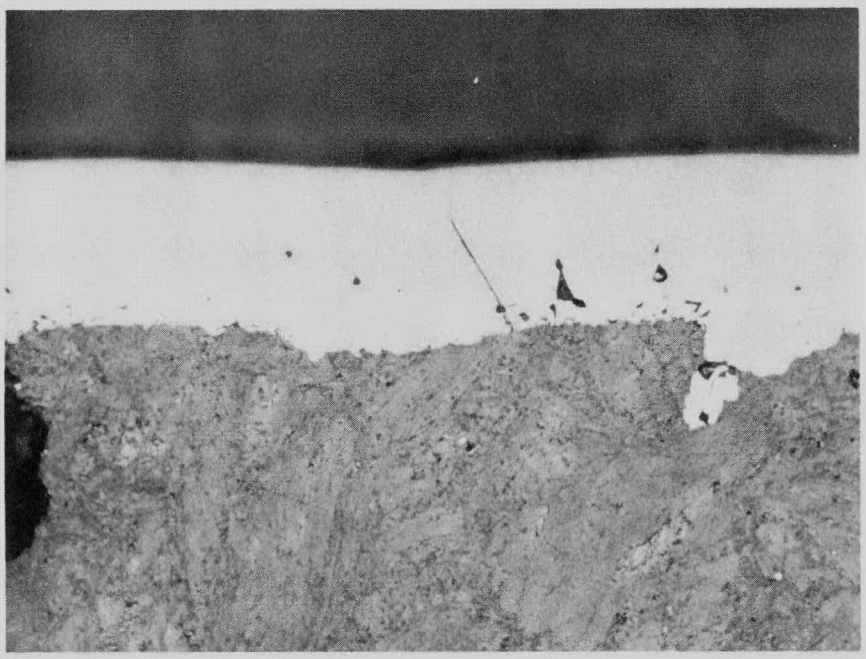

500X Unimpregnated N41102

FIGURE 20. ZrC COATINGS ON ATJ GRAPHITE

DECLASSIFIED 2-28

TABLE 3. LEACHING OF UNIFORMLY LOADED GRAPHITE

Specimen	Halide	Temperature, C	Time, hr	Pressure, mm of mercury	Residual Uranium Content[a], weight per cent	Loss, per cent
A	$ZrCl_4$	1950	1	5	4.1	43
B	$NbCl_5$	1950	1	50	3.7	48.5
C	$NbCl_5$	1950	1	50	1.75	75.0

(a) Analysis of the heated section of the rod.

As expected, the loss of uranium from homogeneously loaded graphite was, in general, less than from surface-impregnated material. However, the lack of agreement between the results of the Runs, B and C, under presumably identical conditions deserves further investigation.

Since the leaching is a surface phenomenon, presumably controlled by the rate of diffusion of uranium through the graphite, the net loss would be expected to decrease as the specimen size is increased. It may also be possible to decrease the loss of uranium by "buffering" the coating vapor feed with an appropriate concentration of uranium halide.

Diffusion of Carbon in Carbides

As was noted above, coating of the blowpipe specimens was carried out under conditions designed to control the over-all rate by the rate of diffusion of carbon through the carbide. Ideally, it should be possible to obtain diffusion constants from the rate of coating formation. However, it is possible to obtain only lower limiting values from the coating data since, although the time-temperature schedule of heating the vaporizer was known in each case, it was not certain when vaporization of the halide under appropriate conditions had started and stopped. Moreover, to the extent that other factors (such as mass-transfer at the vapor-solid interface) may have effected partial control, the coating data give only minimum values for the diffusion rate.

Thus, after the limiting pressures for metal and carbide formation had been determined toward the end of the contract period, it was decided to attempt diffusion measurements in the coating equipment for small rod specimens (see Appendix A). In this equipment, vaporization can be initiated and the specimen heated and cooled quickly so that the time at coating temperature is known. Moreover, it was found that, with suitable precautions, it was possible to follow the progress of the coating by monitoring the electrical conductivity of the resistively heated specimen.

DECLASSIFIED

If diffusion of carbon through the carbide is actually controlling, the coating rate follows a parabolic function:

$$d = k\sqrt{t} ,$$

where d is the coating thickness (assuming a plane surface), k is a constant, and t is the time. If the over-all rate were controlled by mass transfer at the vapor interface, the rate would be linear with time. Thus, it is assumed that, if the coating rate is parabolic, it is characteristic of the diffusion of carbon through the carbide.*

It can be shown[8] that diffusion for cases of this type occurs according to the relation

$$y = \frac{d}{2\sqrt{Dt}} ,$$

where y is a complex function of the concentration gradient through which diffusion takes place. D is the coefficient of diffusion in the fundamental diffusion equation:

$$\frac{dC}{dt} = \frac{\partial}{\partial x}\left(D\frac{\partial C}{\partial x}\right) .$$

Since no data are available on the solubilities of carbon in NbC, TaC, and ZrC with which to evaluate y and, therefore, D explicitly, it is necessary to use the equation in the form: $Dy^2 = \frac{d^2}{4t}$ for the interpretation of the data. Now, if the concentration gradient does not vary with temperature, a plot of log Dy^2 versus 1/T will give the true value of the activation energy for diffusion. Moreover, if it can be assumed that the same carbon concentration gradient exists in the coating process as in the attack of the coated specimen, for example by hydrogen reacting with the diffusing carbon, the diffusion data from the coating experiments can be applied directly to the corrosion problem.

Experimental Work

The principal difficulty with obtaining the required data in the small coating apparatus was that of providing vapor-flow rates sufficiently high to avoid mass-transfer control at the vapor-solid interface and permit the observation of solid-solid diffusion control. By using a large supply of halide in the vaporizer section, a high heat input to the vaporizer, and by eliminating the back pressure (evacuating the condenser section of the tube), it was possible to obtain parabolic growth curves of the type shown in Figure 21.** At lower heat inputs to the vaporizer, lower linear coating rates were obtained.

*It is also possible to interpret the data on the basis of diffusion of the metal through the carbide. However, since the carbon is the more mobile, it is considered to be the diffusing species.

**The points along these curves were obtained by combining the coating thickness measured at the end of a run with conductivity measurements during the run. Electrical leads were provided to measure the voltage drop across the heated section of the specimen carrying a known current. A quartz-wool plug was used to prevent entrainment of solid halide particles.

DECLASSIFIED 2-30

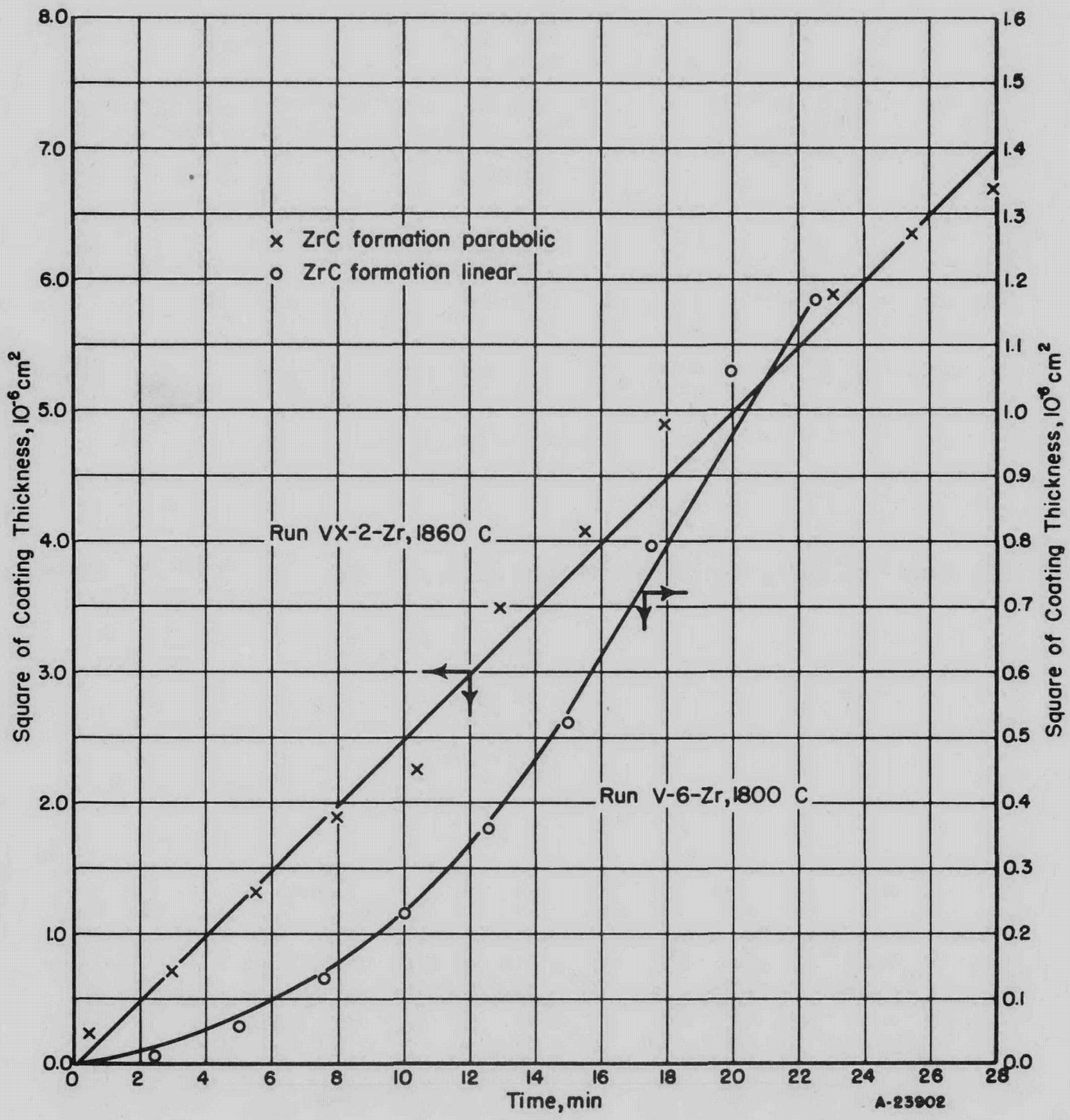

FIGURE 21. ZrC COATING THICKNESS AS A FUNCTION OF TIME

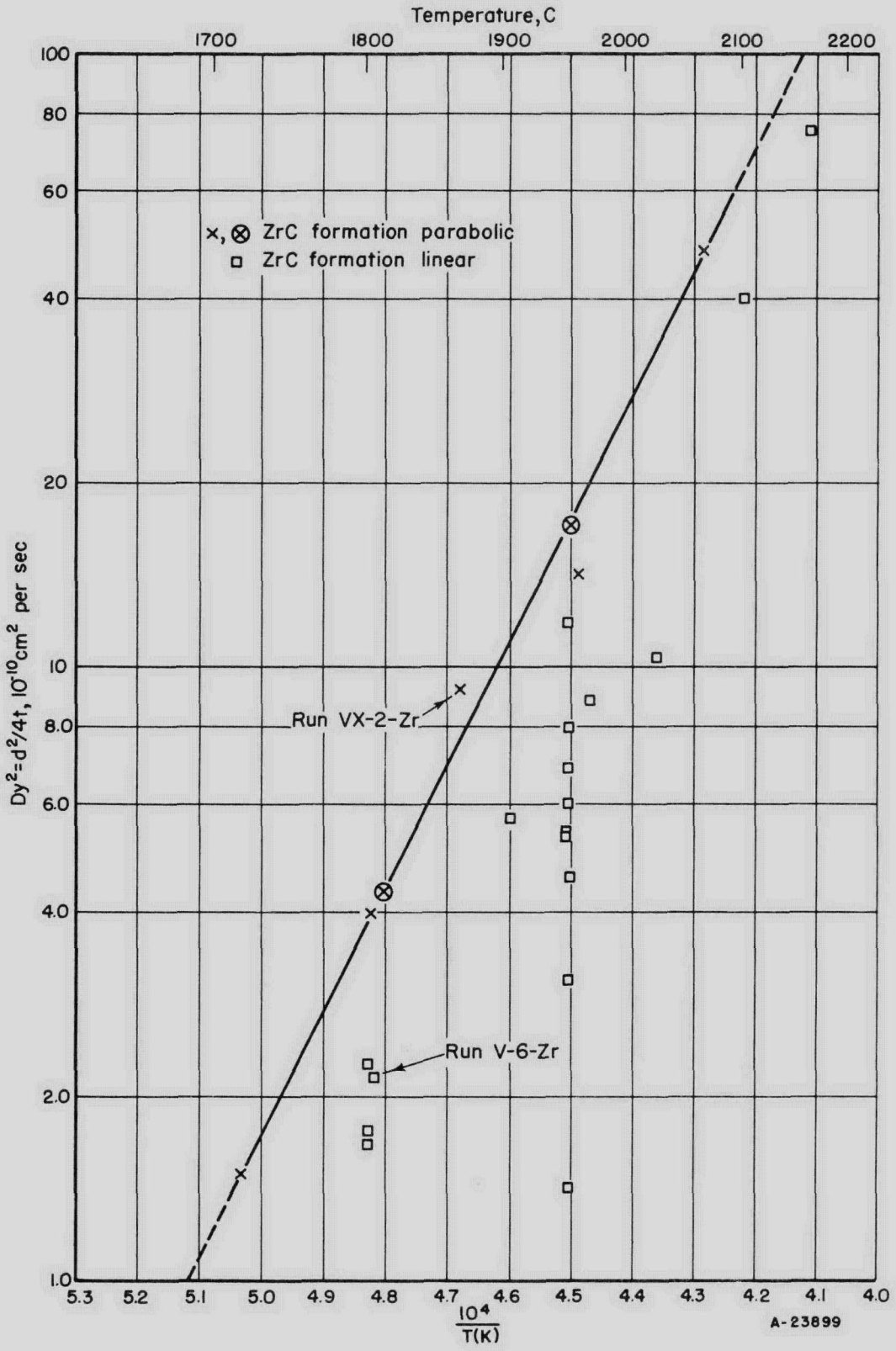

FIGURE 22. ZrC COATING RATE AS A FUNCTION OF TEMPERATURE

DECLASSIFIED 2-22

Figure 22 shows the coating rate as a function of temperature for the formation of ZrC by the thermal decomposition of $ZrCl_4$. As would be expected, the linear, or vapor-flow-controlled rates are all below the parabolic rates.

It appeared that, at the high vapor-flow rates, and despite the evacuation of the condenser section of the tube, the pressure below the vapor barrier and in the region of the specimen was in the range favorable to carbide formation, but unfavorable to metal deposition, e.g., above 0.8 mm of mercury at 2100 C. This was checked by making two runs with a back pressure of 2 mm which is well within the desired range (see Figure 3). The results (encircled points in Figure 22) confirmed those obtained with the condenser section evacuated to promote maximum vapor flow.

The equation for the rate of ZrC formation, which presumably represents the rate of diffusion of carbon through the carbide is:

$$\log_{10} Dy^2 = -\frac{20,000}{T} + 0.24.$$

The indicated activation energy of 91.5 kcal falls between the values 108 kcal and 59 kcal given respectively by Andrews and Dushman[9] and by Pirani and Sandor[10] for the diffusion of carbon through W_2C. A discussion of the discrepancy between the values for W_2C is beyond the scope of this report.

Investigation of the corresponding niobium system was inconclusive at the end of the contract period. Several anomalous results were obtained, and it is not certain that the rates of coating formation were controlled by the diffusion of carbon through the carbide. Additional research would be required to obtain reliable information on the diffusion of carbon through NbC.

ACKNOWLEDGMENT

From time to time, during the course of this research, Battelle staff members other than the authors have given valuable aid which is gratefully acknowledged. J. A. Hoess, H. F. Carlton, E. A. Beidler, D. G. Black, and J. F. Hannah contributed to the final design, construction, and operation of the coating equipment, while Miss V. M. Sheipline aided in the limiting-pressure determinations.

REFERENCES

(1) Powell, C. F., Campbell, I. E., and Gonser, B. W., Vapor Plating, John Wiley & Sons, New York (1955).

(2) Van Arkel, A. E., Metallwirtschaft, 13, 405-408 (1934).

(3) Brewer, Leo, and Krikorian, Oscar, UCRL-2888.

(4) Van Arkel, C. E., Reine Metalle, Julius Springer, Berlin (1939).

(5) Schwarzkopf, Paul, Refractory Hard Metals, The MacMillan Company, New York (1953).

(6) Goldschmidt, H. J., J. Iron Steel Inst., 160, 345 (1948).

(7) Ellinger, F. H., Trans. ASM, 31, 89 (1943).

(8) Crank, J., The Mathematics of Diffusion, Oxford, Clarendon Press (1956).

(9) Andrews, M. R., and Dushman, S., J. Phys. Chem., 29, 462 (1925).

(10) Pirani, M., and Sandor, J., J. Inst. Metals, 73, 385 (1947).

JMB:CJI:DPL:LFP:IEC/ims

DECLASSIFIED 2-34

microfilmed

APPENDIX A

APPARATUS AND PROCEDURE FOR LIMITING-PRESSURE DETERMINATIONS

The apparatus consisted of two identical units mounted side by side, utilizing the same electrical system, vacuum source, surge tank, and gettering furnace. The units were operated alternately. Filament temperatures were measured with an optical pyrometer.

Figure A-1 shows Unit 1 in operation. Figure A-2 shows Unit 2, with a hot-wire filament, being evacuated prior to charging with halide. Figure A-3 shows the electrode assembly with a carbon rod. The corresponding electrode assembly for metal deposition can be seen in the reaction tube in Figure A-2.

Since the vacuum requirements for the apparatus were nominal, a rubber-stopper closure was used for simplicity and flexibility. However, because of leakage resulting from the lack of radial symmetry of the Vycor tubing, it was necessary to provide an auxiliary closure having a truly circular opening. The stainless steel head adopted for this purpose was fitted with a rubber O-ring, which was compressed against the outer wall of the tubing to accommodate the ellipticity and give an adequate seal.

The desired electrode assembly was placed in the reactor, as shown in Figure A-2, which was evacuated to about 10 μ pressure. The pressure within the tube was then adjusted to atmospheric by helium which had been passed over a zirconium getter to remove traces of oxygen, nitrogen, and water vapor.

The electrode assembly was removed and the reaction tube charged with the desired metal halide through a glass tube attached to a charging bottle. After the electrodes were replaced and connected, the liquid-nitrogen trap before the vacuum pump was charged and water routed to the condenser on the reaction tube. The reaction-tube furnace, Figure A-1, was positioned and connected and the system again evacuated.

When the pressure in the system reached 10 μ or less, gettered helium was added to reach the desired operating pressure. The furnace surrounding the reaction tube was heated to a temperature slightly above the dew point of the halide. This prevented premature condensation of the halide on the walls. The bottom furnace was powered by a Variac operating through a Micromax controller, set at the temperature where the vapor pressure of the halide slightly exceeded the adjusted helium pressure in the tube. The filament or rod temperature was adjusted by a Variac, and the temperature of the filament was measured by an optical pyrometer* focused through the slit shown in Figure A-1.

The current increase caused by metal or carbide deposition was measured by the ammeter shown in Figure A-1. The filament temperature at which the rise occurred and the system pressure were recorded.

*Final temperatures were adjusted for emissivity and absorption by the Vycor tube wall.

DECLASSIFIED 2-35

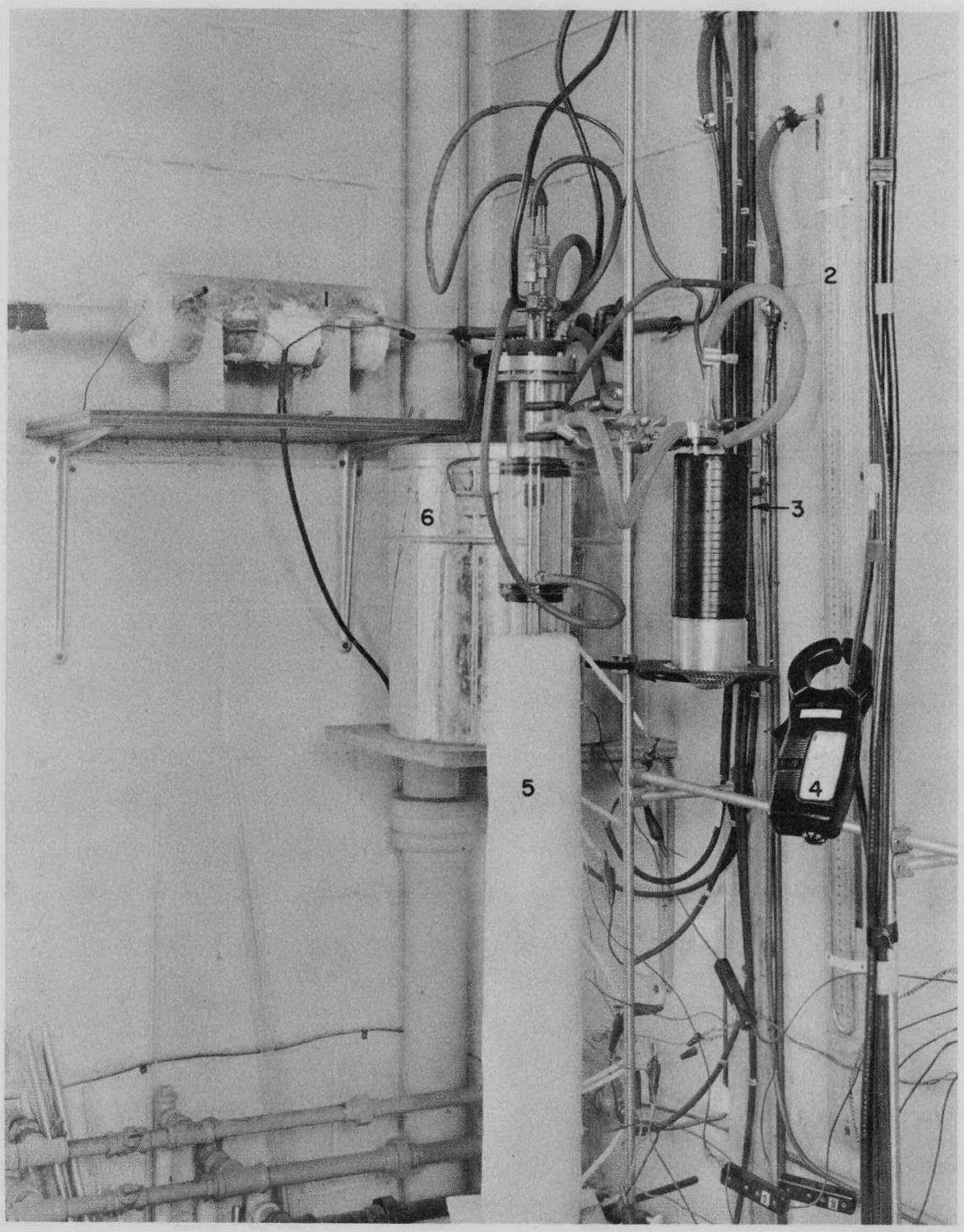

N40675

1. Gettering furnace
2. Manometer
3. Liquid nitrogen trap
4. Ammeter
5. Furnace with electrical and thermocouple leads attached
6. Surge Tank

FIGURE A-1. LIMITING-PRESSURE EQUIPMENT IN OPERATION

2-36

DECLASSIFIED

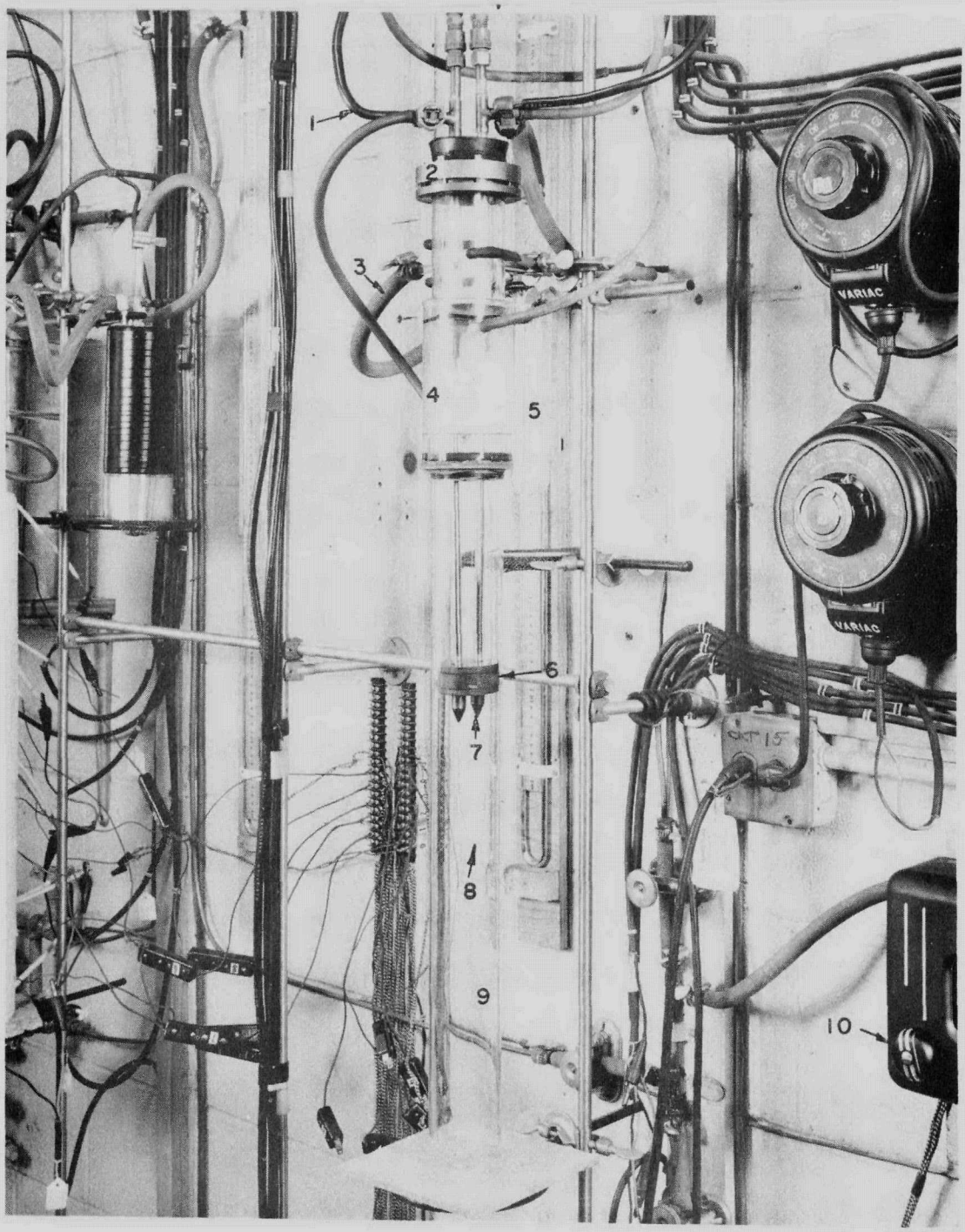

N40673

1. Electrical lead for heating element
2. O-ring vacuum head
3. Vacuum line
4. Water-cooled condenser
5. Trap
6. Split-ring vapor barrier
7. Molybdenum adaptor
8. Wire filament
9. Vycor reaction tube
10. McLeod gage

FIGURE A-2. LIMITING-PRESSURE EQUIPMENT SHOWING FILAMENT ASSEMBLY IN PLACE

DECLASSIFIED 2-37

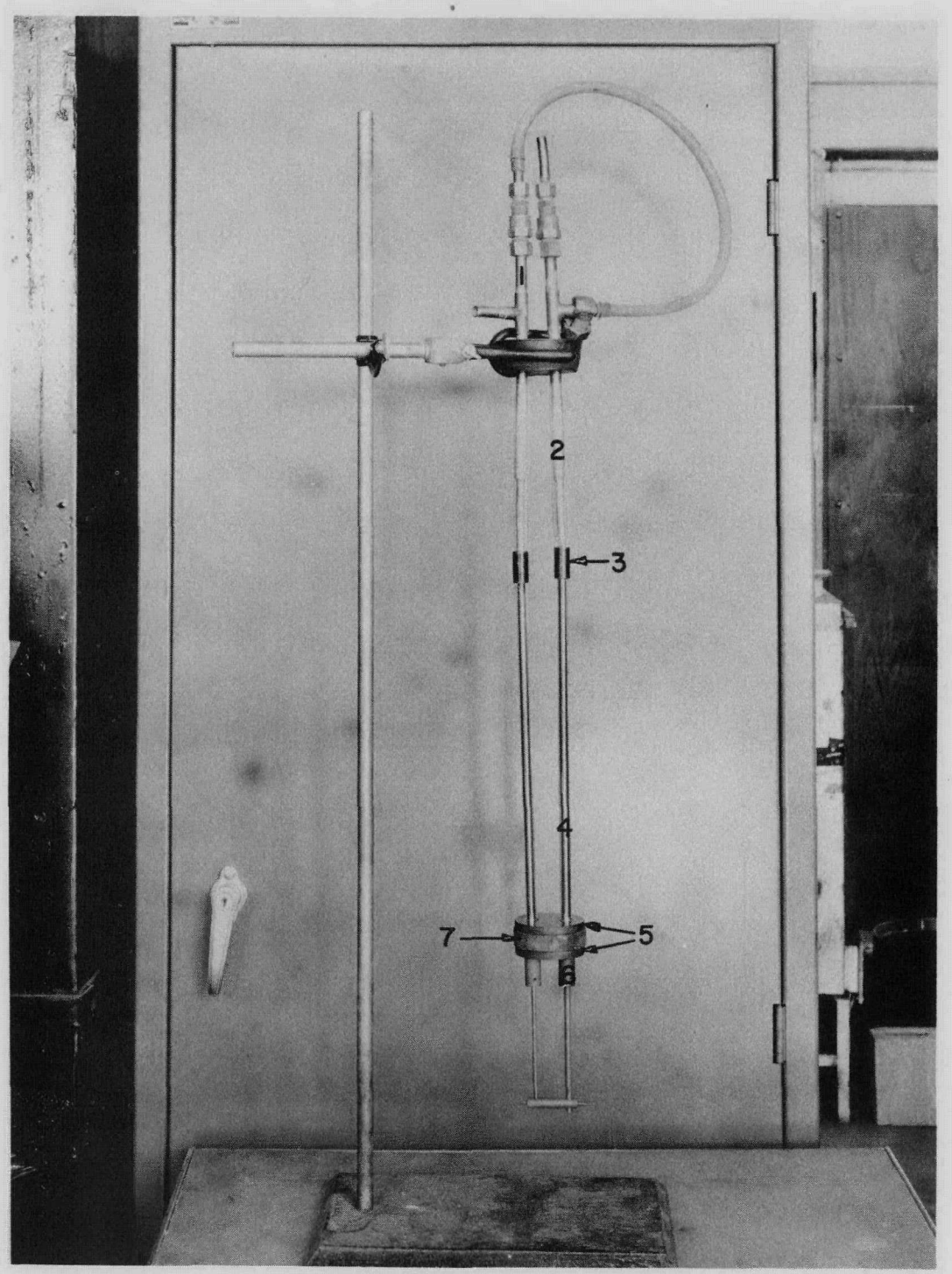

N40620

1. Water-cooled electrodes
2. Pyrex tubing shielding
3. Molybdenum adaptors
4. Molybdenum legs in Pyrex tubing
5. Vycor plates
6. Carbon adaptors
7. Carbon expansion ring (vapor barrier)

FIGURE A-3. GRAPHITE-ROD ASSEMBLY FOR LIMITING-PRESSURE MEASUREMENT

2-38

DECLASSIFIED

It may be asked whether the vapor barrier shown in Figures A-2 and A-3 was effective in maintaining a saturation partial pressure of halide vapor in the region of the filament without introducing a significant pressure drop. Its effectiveness is evidenced by the consistency of the data of Figures A-4 through A-10, taken over several runs for each system in which the vaporization rates varied over an appreciable range.

It will be noted that, for the deposition of zirconium from $ZrCl_4$, it was necessary to work in the liquid range on a tungsten filament. The magnitude of the effect of alloying with the tungsten was not determined. Alloying would be expected to reduce the activity and make deposition in the alloy more favorable than deposition of pure metal, i.e., the experimentally determined limiting pressure would be on the high side.

DECLASSIFIED 2-3-9

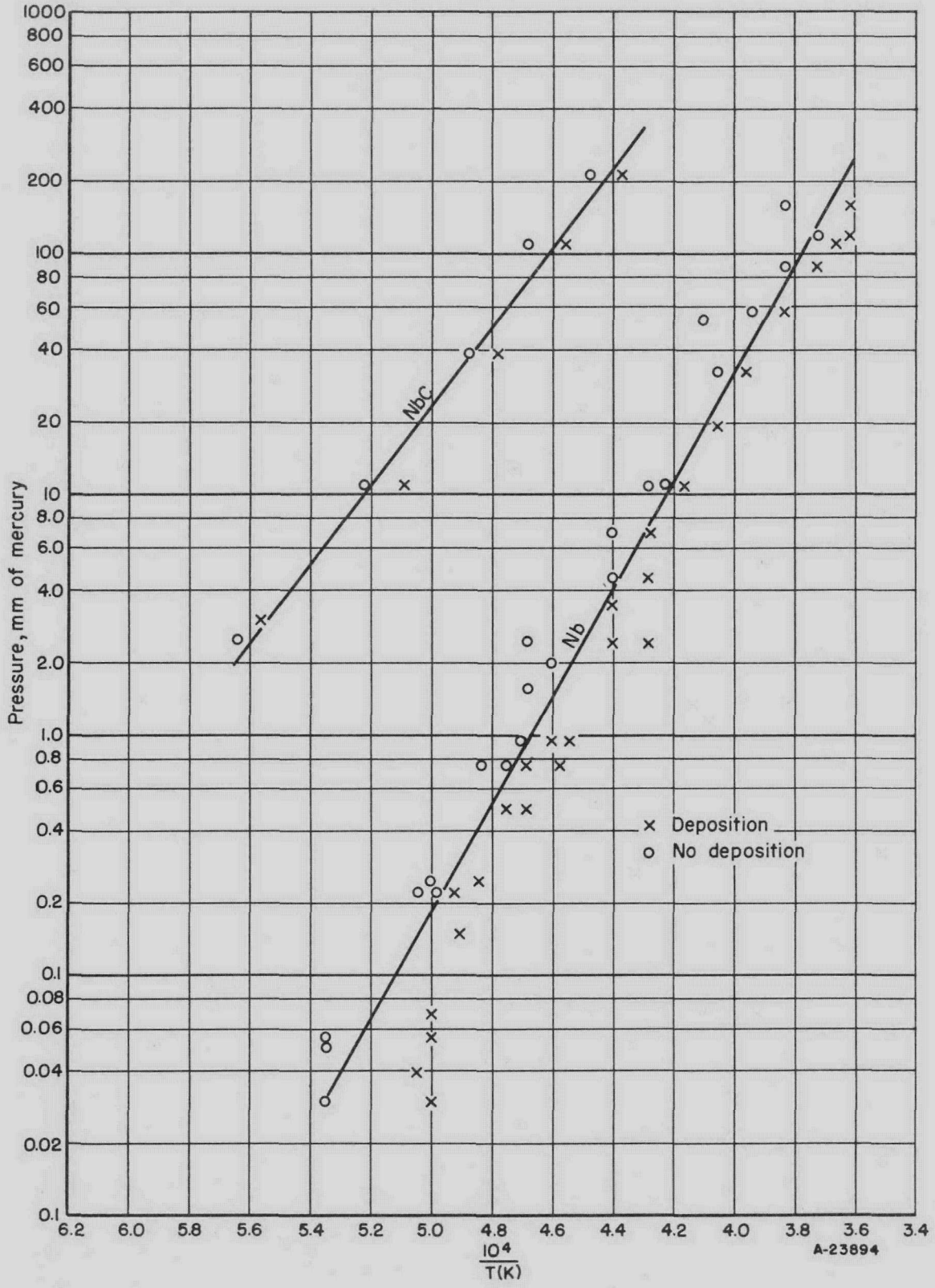

FIGURE A-4. CARBIDE FORMATION AND METAL DEPOSITION FROM $NbCl_5$

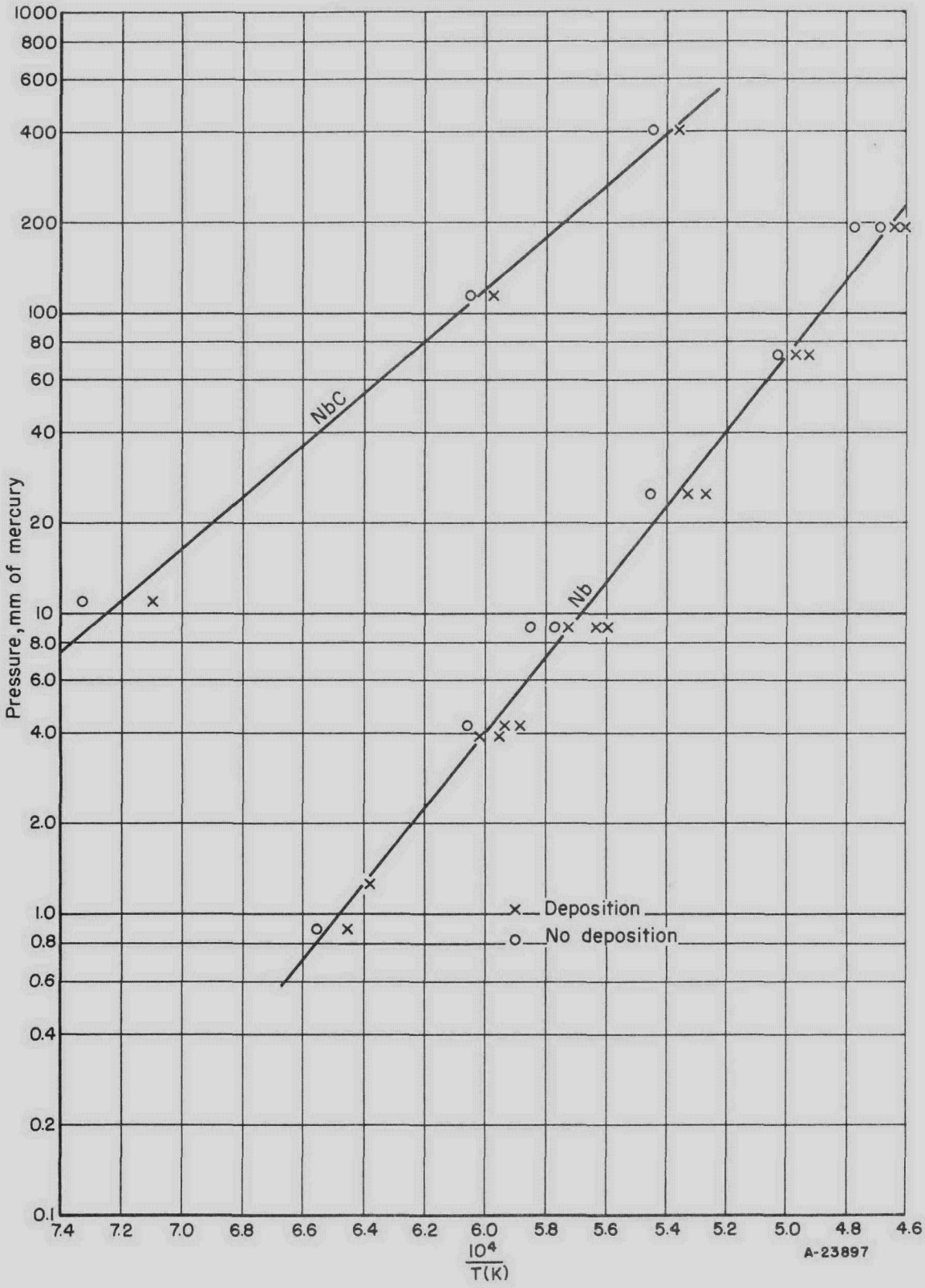

FIGURE A-5. CARBIDE FORMATION AND METAL DEPOSITION FROM $NbBr_5$

DECLASSIFIED

2-41

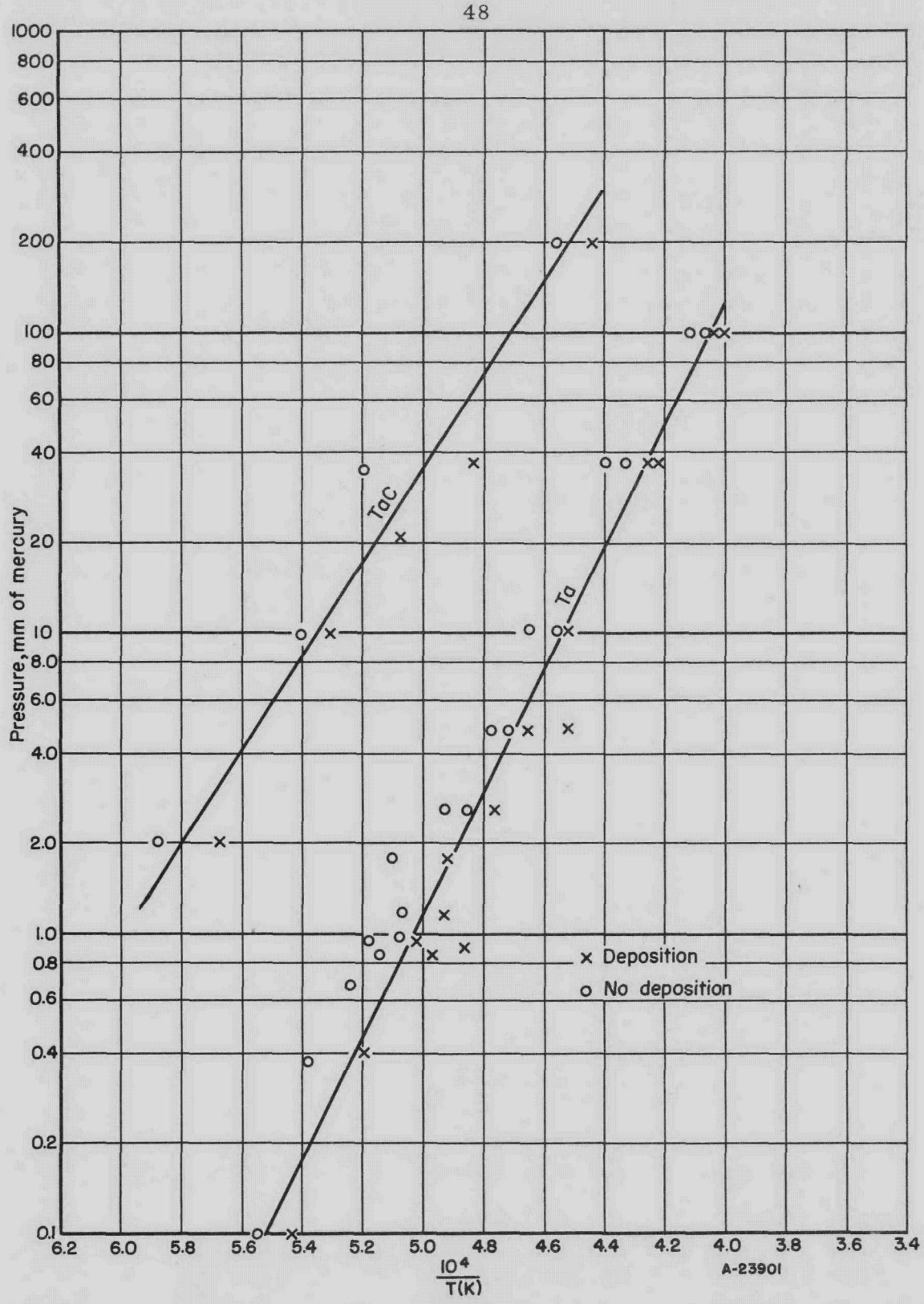

FIGURE A-6. CARBIDE FORMATION AND METAL DEPOSITION FROM $TaCl_5$

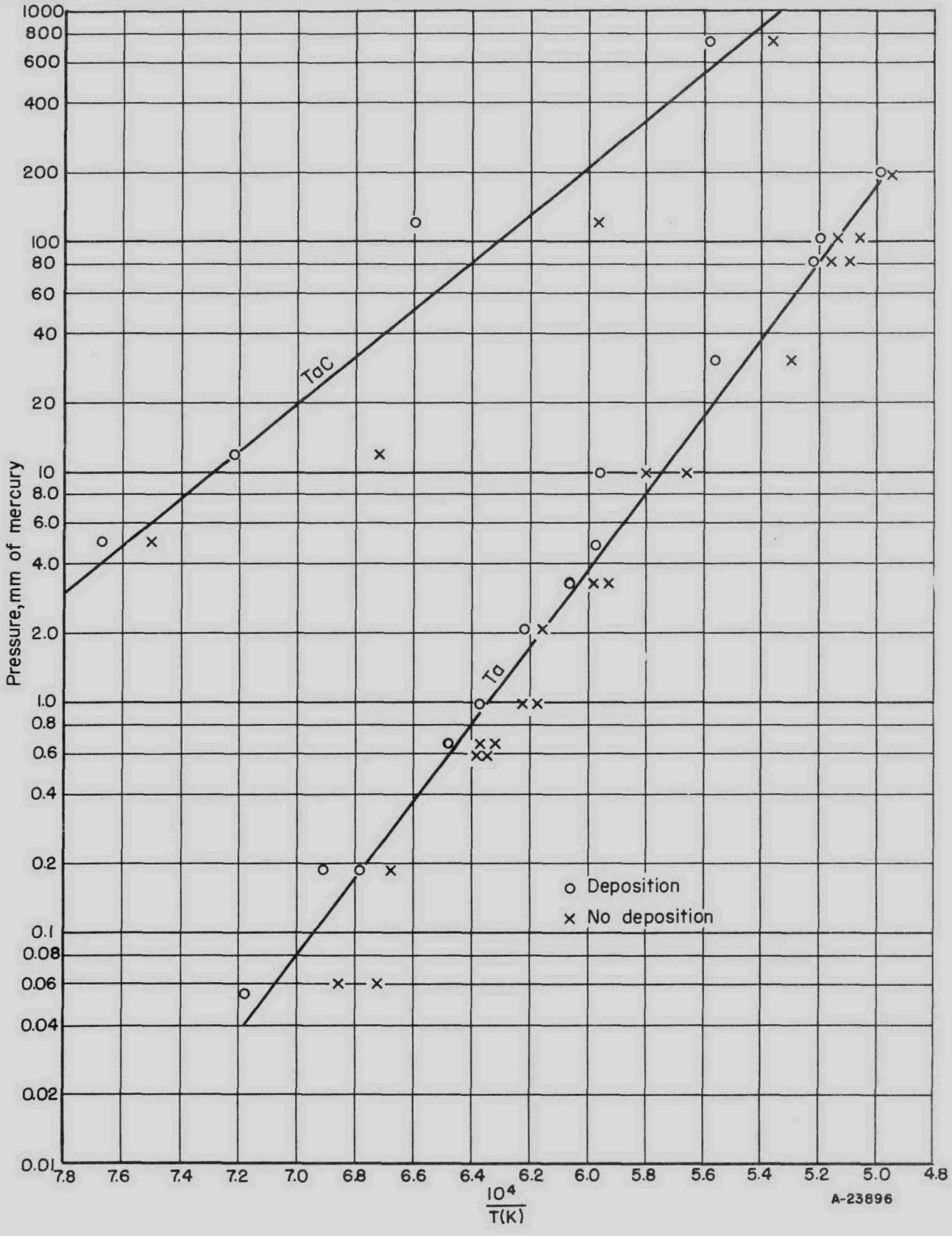

FIGURE A-7. CARBIDE FORMATION AND METAL DEPOSITION FROM $TaBr_5$

DECLASSIFIED

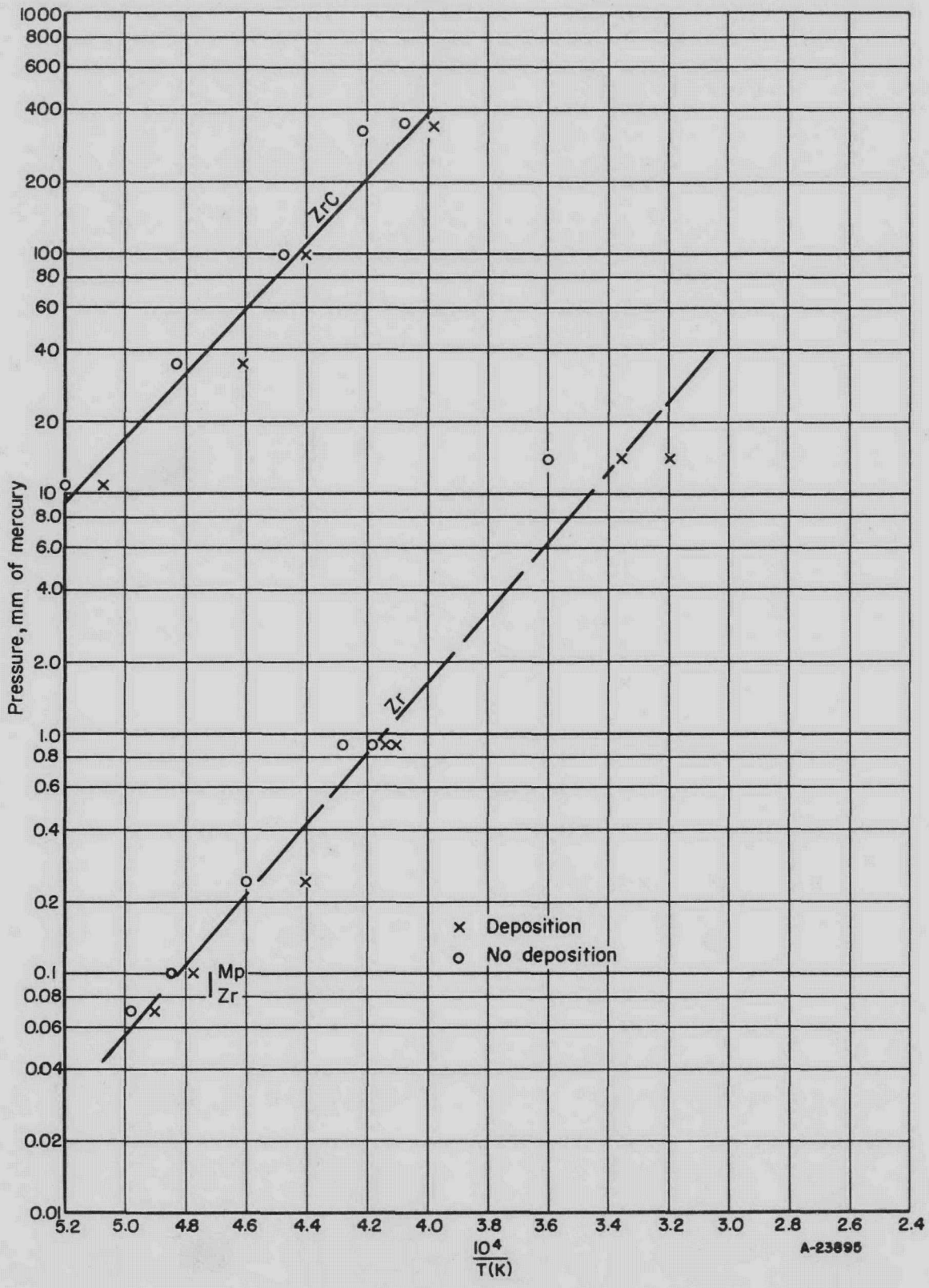

FIGURE A-8. CARBIDE FORMATION AND METAL DEPOSITION ON TUNGSTEN WIRE FROM $ZrCl_4$

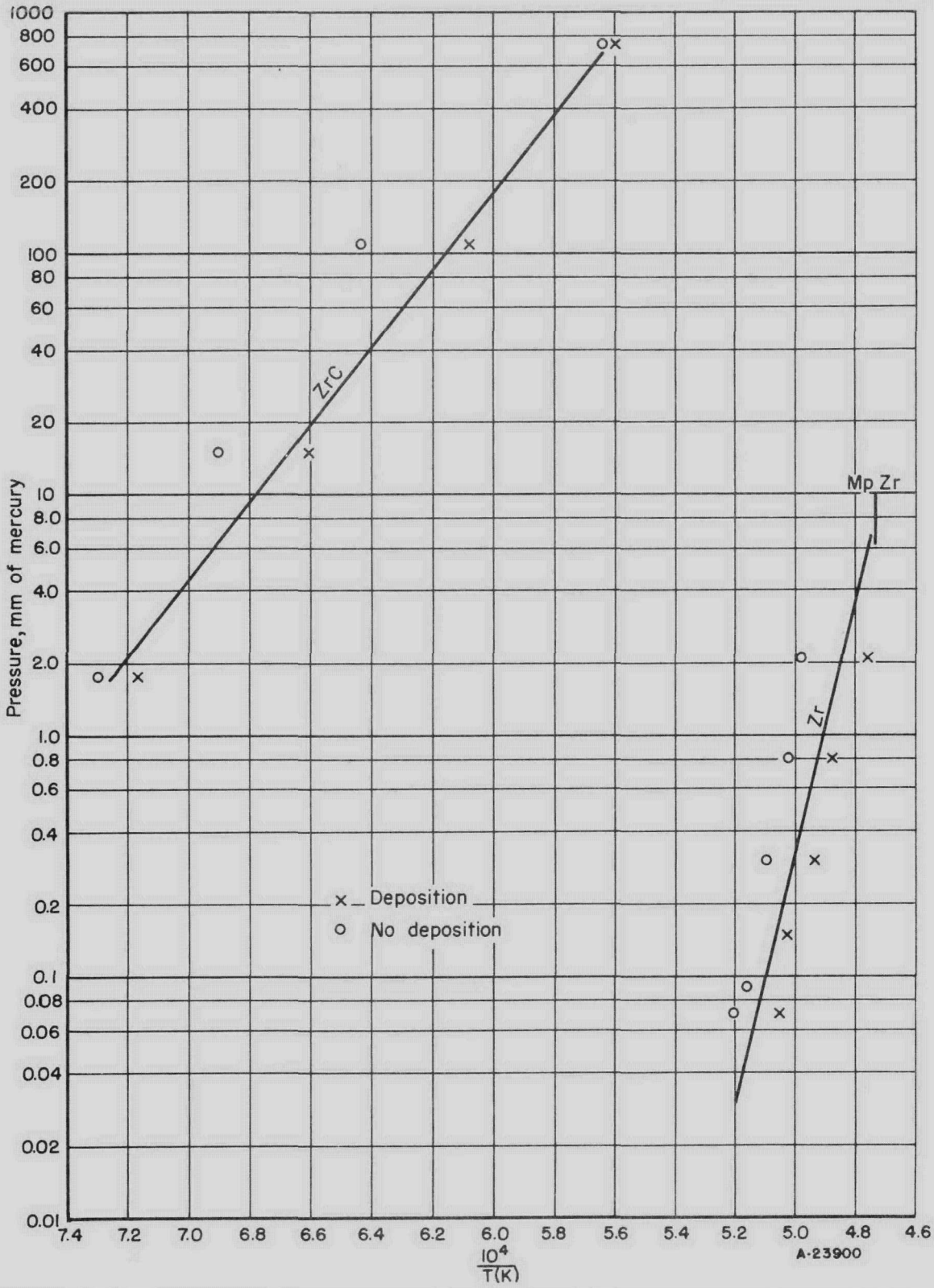

FIGURE A-9. CARBIDE FORMATION AND METAL DEPOSITION FROM $ZrBr_4$

DECLASSIFIED

2-45

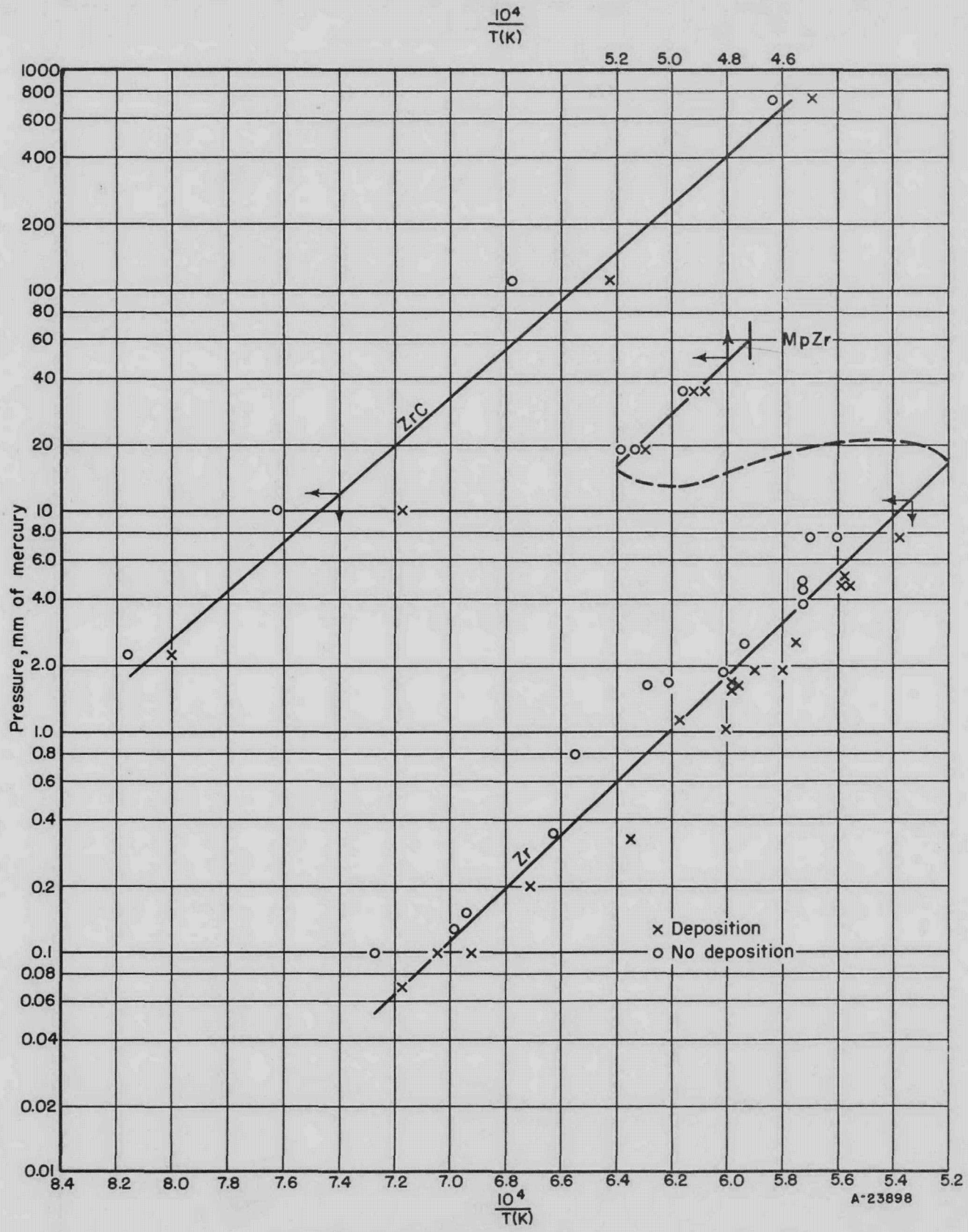

FIGURE A-10. CARBIDE FORMATION AND METAL DEPOSITION FROM ZrI_4

2 46

APPENDIX B

COATING OF BLOWPIPE SPECIMENS

Material

With the exception of zirconium chloride, which was purchased from the Stauffer Chemical Company, the halides used in this work were synthesized from the elements, using high-purity materials. All were handled under an inert-gas blanket.

Apparatus

The coating equipment is described generally in the body of this report. Several details of interest are discussed here.

Heating Circuits

The specimen was heated by a thyratron-controlled Ignitron-fed transformer unit having a capacity of 2100 amp at 29 v, made by the Federal Welding and Machine Company.

The vaporizer circuit was fed by a Transtat-controlled transformer system having a capacity of 500 amp at 15 v.

It was found that at least 1060 amp could be carried by 1/4-in. copper tubing (0.032-in. wall) cooled by tap water at 42 gal per hr. The 36 F temperature rise of the water flowing through a 5-ft length corresponded to a power loss of 3.7 kw. A tubing diameter of 3/8 in. was used in construction of the coating equipment, although the 1/4-in. tubing would have been adequate.

Vacuum System and Pressure Control

The coating equipment was evacuated by means of a Cenco Hypervac-25 pump through a liquid nitrogen-cooled trap and a glass-wool filter designed to catch entrained halide particles. An adjustable mercury manometer provided with electrical contacts and an electronic relay was used to control the pressure in the units by operating a solenoid valve which permitted intermittent pumping of an inert gas bleed.

Typical Data

Tables B-1, B-2, and B-3 give typical data taken from Runs 13331-28-78LM, 13331-19-75LF, and 13331-73-93LF, respectively. Variations in coating thickness were obtained by varying the quantities of halide charged to the vaporizer.

DECLASSIFIED

TABLE B-1. DATA FROM RUN 13331-28-78LM

Halide	$NbCl_5$
Weight of Charge	255 g
Pressure	50.0 mm of mercury
Coating Temperature	2000 C

Time	Specimen Current, amp	Shield Temperature, F	Vaporizer Current, amp	Vaporizer Temperature, F	Remarks
0930	--	--	--	--	Unit assembled and evacuated
1010	65	--	--	--	Specimen fired and pressure brought to 50.0 mm of mercury with helium
1015	440	--	--	--	Power raised to specimen
1025	445	--	--	--	--
1035	440	--	--	--	--
1045	440	--	--	120	--
1050	440	--	--	125	Vaporizer coolant drained
1055	440	1400	160	160	Vaporizer fired
1100	445	--	160	385	--
1105	450	--	165	460	---
1110	450	1410	165	470	--
1120	455	--	185	490	Vaporizer power raised
1130	460	1440	200	520	Vaporizer power raised
1140	465	--	215	570	Vaporizer power raised
1150	470	1440	235	630	Vaporizer power raised
1155	475	--	235	650	--
1200	--	--	--	--	All power off
1300	--	--	--	--	Pressure brought with helium to atmospheric and unit opened

2-48

TABLE B-2 DATA FROM RUN 13331-19-75LF

Halide	$TaCl_5$
Weight of Charge	395 g
Pressure	100 mm of mercury
Coating Temperature	2000 C

Time	Specimen Current, amp	Shield Temperature, F	Vaporizer Current, amp	Vaporizer Temperature, F	Remarks
0900	--	--	--	--	Unit assembled and evacuated
0945	65	--	--	--	Specimen fired
0950	460	--	--	--	Pressure brought to 100.0 mm of mercury with helium, power raised
1000	445	--	--	--	--
1010	440	--	--	--	--
1020	440	--	--	130	--
1025	440	1400	--	150	Vaporizer coolant drained
1030	440	--	160	200	Vaporizer fired
1040	445	--	100	490	Vaporizer power raised
1050	455	1410	185	550	--
1100	460	--	200	565	Vaporizer power raised
1110	465	1420	205	600	--
1120	465	--	230	660	Vaporizer power raised
1125	465	1440	250	710	Vaporizer power raised
1130	465	--	250	735	--
1135	--	--	--	--	All power off
1230	--	--	--	--	Pressure brought to atmospheric with helium and unit opened

DECLASSIFIED 2-49

TABLE B-3. DATA FROM RUN 13331-73-93LF

Halide	$ZrCl_4$
Weight of Charge	170 g
Pressure	5.0 mm of mercury
Coating Temperature	2000 C

Time	Specimen Current, amp	Shield Temperature, F	Vaporizer Current, amp	Vaporizer Temperature, F	Remarks
1030	--	--	--	--	Unit assembled and evacuated
1115	--	--	--	--	Pressure brought to 5.0 mm of mercury with helium
1120	65	--	--	--	Specimen fired
1125	430	--	--	--	Power raised
1135	425	--	--	--	--
1145	420	--	--	--	--
1155	420	1410	--	150	Vaporizer coolant drained
1200	420	--	165	230	Vaporizer fired
1210	420	1440	195	560	--
1220	420	--	205	615	Vaporizer power raised
1230	425	1470	210	645	--
1240	425	--	220	675	--
1250	430	1470	220	700	--
1300	430	--	240	715	Vaporizer power raised
1310	430	1460	240	780	--
1320	--	--	--	--	All power off
1415	--	--	--	--	Pressure brought to atmospheric with helium and unit opened

Atmospheric-Pressure Coater

Runs 11661-50-1LM through 12416-47-19LF were made in a coating unit consisting of separate vaporizing, coating, and condensing chambers which was later abandoned. Difficulty was experienced in obtaining a vacuumtight, electrically insulated seal which would operate at the halide vaporization temperature, and accommodate the thermal expansion of the specimen. Consequently, use of the unit was limited to ZrC coating from ZrI_4 where atmospheric pressure could be used. Unfortunately, this pressure is so close to the limiting pressure for metal deposition that, on occasion, convection currents, sweeping inert gas into the coating region, lowered the partial pressure of ZrI_4 to the point that liquid zirconium formed and ran down the specimen. Some success was obtained when care was taken to avoid mixing of the vapor stream with the inert-gas blanket.

DECLASSIFIED 2-54

APPENDIX C

THERMODYNAMIC ANALYSIS OF PRESSURE RANGE FOR METAL-FREE CARBIDE FORMATION

Consider a simple example in which the metal halide MX_5 dissociates to form the metal and halogen atoms*:

$$MX_5(g) = M(s) + 5X(g). \qquad (C-1)$$

Consider further that one lower halide, $MX_n(g)$ is stable, and that the equilibrium

$$MX_n(g) = M(s) + nX(g) \qquad (C-2)$$

must be considered. At total pressures corresponding to the limiting pressure for metal deposition (see Figures 2 or 3), the pentahalide being fed to the hot surface is dissociated to halogen and the lower halide, but metal is neither deposited nor consumed. It seems reasonable to assume that, at the temperatures involved in this work, the vapor consists principally of lower halides and the halogen and that pentahalide (in this case) is unimportant.

Thus, the limiting pressure is defined by Equation (C-2) and the stoichiometry condition:

$$(5-n)P_{MX_n} = P_X,$$

whence,

$$P_{limit} = P_{MX_n} + P_X = (6-n)P_{MX_n}.$$

From Equation (C-2),

$$K_2 = \frac{P_X{}^n}{P_{MX_n}} = (5-n)^n P_{MX_n}^{n-1}$$

or

$$P_{MX_n} = \frac{K_2^{\frac{1}{n-1}}}{(5-n)^{\frac{n}{n-1}}},$$

and

$$P_{limit} = \frac{(6-n)}{(5-n)^{\frac{n}{n-1}}} K_2^{\frac{1}{n-1}}.$$

*It can be shown that at the temperatures and pressures of interest in this work, the halogens in question are predominantly monatomic.

DECLASSIFIED 2-52

In logarithmic form:

$$\log P_M = \log f(n) + \frac{1}{n-1} \log K_2^*, \qquad (C-3)$$

where P_M is the limiting pressure for metal deposition. Now, in the formation of carbide, the same stoichiometry condition holds at the limiting pressure and Equation (C-2) is replaced by Equation (C-4):

$$MX_n(g) + C(s) = MC(s) + nX(g). \qquad (C-4)$$

Since the gaseous constituents are the same, we have, corresponding to Equation (C-3),

$$\log P_{MC} = \log f(n) + \frac{1}{n-1} \log K_4, \qquad (C-5)$$

and

$$\log P_M/P_{MC} = \frac{1}{n-1} [\log K_2 - \log K_4], \qquad (C-6)$$

or

$$\log P_M/P_{MC} = \frac{1}{n-1}\left(\frac{-\Delta F_2 + \Delta F_4}{2.303\ RT}\right). \qquad (C-7)$$

It will be noted that Equations (C-2) and (C-4) differ by

$$M(s) + C(s) = MC(s), \qquad (C-8)$$

where $\Delta F_8 = \Delta F_4 - \Delta F_2$ is the free energy of formation of the carbide, ΔF_{MC}, whence:

$$\log P_{MC}/P_M = \frac{\Delta F_{MC}}{(n-1)\ 2.303\ RT}. \qquad (C-9)$$

---

* It should be noted at this point that $\log K_2 = (n-1) \log P_M$ and that $(n-1) \frac{d \log P_M}{d(1/T)} = -\frac{\Delta H_2}{2.303\ R}$.